

1-1-2005

The design and testing of a hydrogen fueled internal combustion engine

Evangeline Bulla

University of Nevada, Las Vegas

Follow this and additional works at: <https://digitalscholarship.unlv.edu/rtds>

Repository Citation

Bulla, Evangeline, "The design and testing of a hydrogen fueled internal combustion engine" (2005). *UNLV Retrospective Theses & Dissertations*. 1928.

<http://dx.doi.org/10.25669/wzj7-dq2p>

This Thesis is protected by copyright and/or related rights. It has been brought to you by Digital Scholarship@UNLV with permission from the rights-holder(s). You are free to use this Thesis in any way that is permitted by the copyright and related rights legislation that applies to your use. For other uses you need to obtain permission from the rights-holder(s) directly, unless additional rights are indicated by a Creative Commons license in the record and/or on the work itself.

This Thesis has been accepted for inclusion in UNLV Retrospective Theses & Dissertations by an authorized administrator of Digital Scholarship@UNLV. For more information, please contact digitalscholarship@unlv.edu.

THE DESIGN AND TESTING OF A HYDROGEN FUELED INTERNAL
COMBUSTION ENGINE

by

Evangeline Bulla

Bachelor of Science
Jawaharlal Nehru Technological University, India
2002

A thesis submitted in partial fulfillment
of the requirements for the

Master of Science Degree in Mechanical Engineering
Department of Mechanical Engineering
Howard R. Hughes College of Engineering

Graduate College
University of Nevada, Las Vegas
May 2006

UMI Number: 1436741

INFORMATION TO USERS

The quality of this reproduction is dependent upon the quality of the copy submitted. Broken or indistinct print, colored or poor quality illustrations and photographs, print bleed-through, substandard margins, and improper alignment can adversely affect reproduction.

In the unlikely event that the author did not send a complete manuscript and there are missing pages, these will be noted. Also, if unauthorized copyright material had to be removed, a note will indicate the deletion.

UMI[®]

UMI Microform 1436741

Copyright 2006 by ProQuest Information and Learning Company.

All rights reserved. This microform edition is protected against unauthorized copying under Title 17, United States Code.

ProQuest Information and Learning Company
300 North Zeeb Road
P.O. Box 1346
Ann Arbor, MI 48106-1346



Thesis Approval
The Graduate College
University of Nevada, Las Vegas

April 13, 2006

The Thesis prepared by

Evangeline Bulla

Entitled

Design and Testing of a Hydrogen Fueled Internal Combustion Engine

is approved in partial fulfillment of the requirements for the degree of

Master of Science in Mechanical Engineering

Examination Committee Chair

Dean of the Graduate College

Examination Committee Member

Examination Committee Member

Graduate College Faculty Representative

ABSTRACT

The Design and Testing of A Hydrogen Fueled Internal Combustion Engine

by

Evangeline Bulla

Dr. Robert Boehm, Examination Committee Chair
Professor of Mechanical Engineering
University of Nevada, Las Vegas

A conventional single cylinder 425 cc four stroke internal combustion Polaris engine has been modified to run on hydrogen gas. For such an effort, both port injection as well as direct injection of hydrogen were attempted on the engine in order to evaluate its performance. The emphasis was placed on using direct injection of hydrogen over port injection, thereby utilizing the benefits of having high potential with regard to power, efficiency and also the minimization of NO_x emissions. The engine was tested at Kell's automotive using a specially designed dynamometer for this purpose. Various performance parameters like power, torque, emissions, etc were evaluated by the installation of different software's like Dynamite, e-com and KAM's. Problems of irregular combustion owing to pre-ignition in the intake and compression phase, knocking combustion and also lower power output as a result of the larger range of flammability were observed during the performance evaluation. Finally, direct injection of hydrogen has been a viable approach on the Polaris engine.

TABLE OF CONTENTS

ABSTRACT	iii
LIST OF FIGURES	v
LIST OF TABLES	vii
ACKNOWLEDGEMENTS	viii
CHAPTER 1 INTRODUCTION	1
Literature Review	2
General Conclusions	11
CHAPTER 2 PHYSICAL DETAILS	12
Testing Equipment	13
Engine and its Modifications	26
CHAPTER 3 PERFORMANCE AND EMISSIONS EVALUATION	44
Engine performance while operating it on gasoline	44
Engine emission evaluation while operating it on gasoline	47
Engine performance while operating it on natural gas	50
Engine emission evaluation while operating it on natural gas	54
Engine performance while running it on hydrogen gas	58
Port injection of hydrogen	58
Direct injection of hydrogen	61
CHAPTER 4 SUMMARY AND CONCLUSIONS	64
APPENDIX I PDF FILES	65
APPENDIX II RUN IDENTIFICATION	75
REFERENCES	80
VITA	83

LIST OF FIGURES

Fig 1	Engine as received	13
Fig 2	Dyno kit	14
Fig 3	Dyno-max 2000™ software	15
Fig 4	Engine on a test stand with the dyno attached.....	16
Fig 5	Crank position bracket.....	17
Fig 6	Engine with crank trigger	18
Fig 7	Engine with crank position sensor.....	18
Fig 8	Engine with cam shaft sensor	19
Fig 9	Throttle position sensor bracket	20
Fig 10	Throttle stop bracket.....	20
Fig 11	Engine with the oxygen sensor.....	22
Fig 12	Engine with thermistor, ECT installed	23
Fig 13	Engine with oil tank, reservoir installed.....	24
Fig 14	Engine with shell and heat tube exchanger	24
Fig 15	Engine with the ignition coil	25
Fig 16	Engine with catalytic converter	26
Fig 17	Assembled intake manifold	27
Fig 18	ABS prototype of intake manifold	28
Fig 19	Manufactured intake manifold with butterfly valve.....	28
Fig 20	Manufactured intake manifold with the fuel injector	28
Fig 21	Engine with four injectors installed.....	29
Fig 22	Engine with Hoerbiger injector	31
Fig 23	Assembled intake manifold with Hoerbiger injector.....	31
Fig 24	Engine with the booster box	32
Fig 25	Assembled throttle body design with the solenoid valve	34
Fig 26	Engine with the second Hoerbiger injector	37
Fig 27	Engine with in-cylinder hydrogen injection by the use of Hoerbiger injector	38
Fig 28	Engine attached with two mass flow meter	40
Fig 29	Engine with solenoid valve attached	40
Fig 30	Engine with solenoid valve attached to the cylinder head.....	41
Fig 31	Design of the solenoid valve with the check valve	42
Fig 32	Comparison of torques at different speeds (gasoline)	45
Fig 33	Comparison of power at different speeds (gasoline).....	47
Fig 34	Comparison of emissions at stoichiometric A/F ratio (gasoline)	48
Fig 35	Comparison of emissions at rich A/F ratio (gasoline).....	48
Fig 36	Comparison of emissions at rich A/F ratio (gasoline).....	50
Fig 37	Comparison of torques at different speeds (natural gas)	52
Fig 38	Comparison of powers at different speeds (natural gas)	53
Fig 39	Comparison of emissions at stoichiometric A/F ratio (natural gas).....	54

Fig 40	Comparison of emissions at lean A/F ratio (natural gas)	56
Fig 41	Comparison of emissions at rich A/F ratio (natural gas).....	57
Fig 42	Comparison of powers at 40:1 A/F ratio (port injection of Hydrogen).....	59
Fig 43	Comparison of torques at 40:1 A/F ratio (PI of hydrogen)	60
Fig 44	Comparison of emissions at 40:1 A/F ratio (PI of hydrogen)	61
Fig 45	Comparison of powers at 20.6 A/F ratio (DI of hydrogen).....	62
Fig 46	Comparison of torques at 20.6 A/F ratio (DI of hydrogen).....	63

LIST OF TABLES

Table 1	Different torques at different speeds (gasoline).....	44
Table 2	Different power output at different speeds (gasoline)	46
Table 3	Emissions at 14.7 A/F ratio (gasoline).....	48
Table 4	Emissions at 13.7 A/F ratio (gasoline).....	49
Table 5	Emissions at 15.7 A/F ratio (gasoline).....	50
Table 6	Different torques at different speeds (natural gas).....	51
Table 7	Different power output at different speeds (natural gas)	53
Table 8	Emissions at 14.5 A/F ratio (natural gas)	54
Table 9	Emissions at 14 A/F ratio (natural gas)	55
Table 10	Emissions at 15 A/F ratio (natural gas)	57
Table 11	Different power output at 40:1 A/F ratio (port injection of hydrogen)	58
Table 12	Different torques at 40:1 A/F ratio (port injection of hydrogen).....	59
Table 13	Emissions at 40:1 A/F ratio (port injection of hydrogen).....	60
Table 14	Different power output at 20:1 A/F ratio (direct injection of hydrogen)...	61
Table 15	Different torques at 20:1 A/F ratio (direct injection of hydrogen)	62
Table 16	Various test run results for gasoline	76
Table 17	Various test run results for natural gas	77
Table 18	Various test run results for hydrogen gas	78

ACKNOWLEDGMENTS

I offer my sincere thanks to Dr. Boehm, project advisor and committee chair, for his guidance, patience and support in the entire work carried out and also the committee members for their co-operation and time. I am very grateful to Ron Fifield, Julian Gardner and the other project members for their help in this work. I would like to thank Terry and Sig Kell at Kell's Automotive for allowing the University to use their shop, for all the guidance and help offered during this work and also the Department of Energy for funding this project. And finally, but not the least, my family members and close friends for the prayers offered and the encouragement given to me throughout the entire period.

CHAPTER 1

INTRODUCTION

This project was funded by the Department of Energy to the University of Nevada Las Vegas and an effort was made to design and test a single cylindered four stroke 425 cc internal combustion Polaris engine which usually runs on gasoline, to make it run on hydrogen gas. The details of Polaris Ranger 2X4 internal combustion engine are included. For pursuing this idea, modifications of the engine have been carried out, so that it would be compatible to run on hydrogen gas.

Hydrogen, even though "renewable" and "clean-burning," does give rise to some undesirable combustion problems in an engine operation, such as backfire, pre-ignition, knocking and rapid rate of pressure increase. It has been experimentally shown that the fuel induction technique does play a very dominant role in obtaining smooth engine operation.

For this project, instead of the conventional port injection approach, emphasis was placed on using direct injection of hydrogen that injects the fuel directly in the combustion chamber at relatively high pressure and can eliminate pre-ignition in the intake manifold, however it does not necessarily eliminate it in the combustion chamber.

It also offers very high potential with regard to power and also the minimization of NO_x emissions. Utilizing the benefits and sources available for hydrogen work at Kell's automotive, the engine work was pursued at the shop under the guidance of Terry Kell.

Furthermore, a decision was made by him to run the Polaris Ranger internal combustion engine on gasoline first and then to natural gas and finally on hydrogen gas and examine the various aspects of the behavior of the engine with regards to power output and emissions.

Literature Review

The project started with a search for information on prior research on such an approach. Many scientists and researchers have carried out work on hydrogen engines.

One such work found in the literature highlighted on the design of the hydrogen supply system by Guo et al. (1999) who employed fast response valves possessing good switching characteristics, as well as hydrogen injectors and a chip microprocessor which controls injection timing optimally thereby improving engine performance. They showed that abnormal combustion such as back-fire, pre-ignition, rate of pressure increase and knock did not occur, and the performance of the engine could be improved by means of the hydrogen injection system with fast response solenoid valves.

Sierens and Verhelst (2003) employed sequential multipoint injection of hydrogen wherein the injector was placed at different angles to the inlet airflow. Results showed that Y-junction injection gave high power output of the engine 1470 W running at 600 constant rpm because of maximum air and fuel flow flowing for a particular start of injection of 80 deg ATDC. Further results showed that the power output changes linearly with the air/fuel equivalence ratio for an optimal ignition timing. The indicated efficiency of the engine was high when there was an increase in the turbulence and better

mixing of the fuel and air, so better combustion results in high efficiency. The back fire phenomenon was not present as they carried the tests at an air to fuel ratio > 1.4 .

DeBoer et al. (1976) used a single-cylinder engine with a fuel injector mounted in the sidewall of the cylinder, about midway between top and bottom and observed that the efficiency of the engine increases with higher compression ratio. With a $\phi < 0.4$, the efficiency of the engine was high but decreased as ϕ increased, and also as the engine speed increased, the efficiency also increased. Series of papers by King and his collaborators (1948-1958) showed that a compression ratio as high as 14 can be used with stoichiometric mixtures provided the cylinder and piston were kept scrupulously clean. Lean operation of hydrogen yielded less NO levels which were about 14 times smaller than peak NO levels of an engine running on gasoline.

Mathur and Khajuria (1984) conducted tests on a Varimax compression engine and showed that a thermal efficiency of 50% was higher at lower equivalence ratio of $\phi < 0.6$. Quality governing with lean mixtures gave higher efficiencies 25-100% and also the advantage of lower NO_x emissions than obtainable with a gasoline engine.

Heffel (2000) modified a 427 Ford FE engine and used a specially designed electronic fuel injection for metering hydrogen. At a $\phi = 0.4$, the NO_x formed was less with maximum power output of 270 hp and a torque of 230 ft-lb. Further, when the effective octane rating increased, it enabled the engine to tolerate compressions of 15:1 at a $\phi = 0.4$. Whereas at chemically correct or stoichiometric mixtures it could tolerate only slightly above 8:1.

Martorano and Dini (1983) employed a direct injection technique for the fueling system of a two stroke reciprocating gas engine. Then proved that to avoid a loss in

specific horsepower, one should employ an engine in which hydrogen is directly injected into the combustion engine after the induction stroke. In order to obtain a satisfactory mixture of hydrogen and air while avoiding pre-ignition, a variety of different types of nozzles have been tried. The best performance was obtained with injections quite before TDC. Larger power rates than those obtainable by a gasoline carburetor engine were accompanied by higher thermal efficiencies.

Helmut et al. (2003) carried out experiments on a single cylinder research engine by using a high pressure injector to achieve both a low injection amount of fuel and also to be able to inject the hydrogen at full load amount in the shortest possible time. The injector was designed in the form of a multi-hole nozzle configuration with an overall cross-section designed in such a way that at low injection pressures the idling amount of fuel was available, and that at high pressures short injection times can be achieved for high-load operating points.

Port Injection

Some experiments were carried out with port injection of gasoline and hydrogen to obtain data on a comparison to the hydrogen direct injection mode. It was seen that while using gasoline as a fuel at partial and full load engine loads there were almost no differences discernible in the combustion period. But with hydrogen under the same conditions it was observed that as the engine load decreased, air fuel ratio increased and thus the combustion period distinctly increases, leading to increased losses due to real combustion. In this case, the combustion period can be shortened by slight throttling because stronger throttling has the disadvantage that the throttling losses exceed the

advantages obtained by the shortened combustion period. It was also observed that hydrogen has outstanding combustion properties compared to gasoline under full load.

Direct Injection of Hydrogen

Other experiments showed that the start of injection had an influence at a speed of 2000 rpm. With the aim of achieving the best efficiency the start of ignition was varied for each engine load within an indicated mean effective pressure range of 5-10 bar. It was noted that at a constant injection pressure, an increase in engine load led to an extension of the injection period. It was necessary to move the latest possible injection time point with increasing load from the initial 40 to 60 ° crank angle BTDC.

Despite higher hydrogen emissions, higher efficiency was achievable. They observed increased production of NO_x due to the increasing combustion temperatures. Burning of rich mixtures led to higher hydrogen emissions, whereas, homogeneous lean mixture burned almost with no NO_x emissions. They observed different efficiencies at different starts of injection mainly due to the different properties of air and hydrogen and also due to different charge mass during compression. Results also showed that there was an increase in the efficiency when the injection took place late, this occurred mainly due to an increase in the mean effective pressure. As the retardation of start of injection took place, it led to an inhomogeneous mixture and consequently due to rich mixture zones the combustion velocity increased.

Emissions

By delaying the start of injection, it was noticed that at higher loads using direct injection, the NO_x emissions reduced drastically because there was barely any time

available for a mixture homogenization, rich and very lean zones formed alternately. Thus they showed that the change in start of injection had a greater impact in the reduction of NO_x emissions. At lower loads, maximum possible mixture homogenization led to the avoidance of NO_x . It was observed that at indicated mean effective pressure of 5.5 with internal mixture configuration the NO_x emissions were equal to zero. They highlighted the fact of using the advantage of non-throttled operation in higher partial load operation. By either the use of lean strategy operation mode or a reduction catalytic converter, both of the variants ensured an approximately emission free operation throughout the entire load and speed range.

Experiments carried out by Ford (2004) on a four cylinder internal combustion supercharged engine was made to run on gaseous hydrogen from light weight composite cylinders. It used a modular hybrid transmission system. In their work a high compression ratio, a super charger and an intercooler were combined to densely pack air into the engine. They tested the engine for pre-ignition limits and the pistons, piston pins and connecting rods were suitably upgraded to handle any pre-ignition events. The 2.3 litre engine was added with a centrifugal supercharger which would boost up to 1 bar, as a result there was an increase in the temperature of the inlet charge. In order to reduce this effect, an air-air intercooler was incorporated into the design. By supercharging, there would be maximum engine power so in order to achieve that, they incorporated with two injectors per cylinder. During low speeds, a low flow rate injector was used and at relatively higher speeds a second larger injector was used alone.

They utilized late fuel injection timing this allowed the induction gases to provide additional cooling to the exhaust valve during valve overlap without introducing

hydrogen directly into the exhaust. It also allowed injecting the fuel only after the exhaust valve has closed in order to minimize the occurrence of back flash. It was observed that the NO_x emissions were extremely low at an equivalence ratio of 0.5 and thereafter increased this was because of the combustion of engine oil. Using the air-air intercooler, at an equivalence ratio of 0.5 reduced the peak torque approximately by 28% compared to gasoline.

A specially designed single cylinder test engine equipped with external and internal mixture formation systems was used by BMW (2004) to investigate the potentials of a combined operation of direct injection and port fuel injection and the effects of various injection pressures were studied. An electromagnetic injector, which has extremely high flow capabilities, was used for this purpose. Simulation tools such as pressure curve analysis and one dimensional flow simulation was used in designing of the test engine. Engine loss analysis was also developed. High thermal efficiency and extremely low NO_x emissions were possible for a low engine load with lean hydrogen mixture when it was delivered unthrottled by external mixture formation. Similarly at higher engine loads NO_x emissions increased and this required stoichiometric operation in order to reduce the NO_x emissions in a catalytic converter. Using a compression ratio of 13 eliminated pre-ignition and also allowed high thermal efficiency at part load and full load operation. It was observed for leaner mixtures NO_x emissions were close to zero whereas for richer mixtures NO_x emissions were at significant levels. At low loads with unthrottled lean operation with external mixture formation the NO_x was equal to 100 ppm, with medium loads operated with throttled stoichiometric external mixture formation there was a

reduction in NO_x in a catalyst same was the case at higher loads with internal mixture formation.

Wimmer et al. (2005) carried out experiments on a four stroke single cylinder, wherein they used direct injection of hydrogen with the help of solenoid injectors as well as piezo driven high-pressure injectors. The injector was positioned between the intake valves. They observed that as the air fuel ratio was increased there was an increase in the combustion duration. An early and late injection timing resulted in a tumble motion. From the experiments it was concluded that the injection should start as late as possible during the compression stroke. It was observed that with hydrogen port injection the efficiency of the ideal engine was higher while with hydrogen direct injection the operating efficiencies were higher. The engine was equipped with 10 surface temperature sensors to the cylinder head in order to investigate wall heat losses. It was observed that the heat transfer coefficients were higher during combustion for hydrogen port injection compared to gasoline operation. With early hydrogen direct injection operation the combustion was symmetrical. Pressure rise and the maximum cylinder pressure were rather low. So, the sensors near the spark plug showed an increase in heat flux. But with late hydrogen direct injection operation there was a very short, intense combustion with higher-pressure increase. Lower air fuel ratio led to lower NO_x emissions and higher air fuel ratio led to higher NO_x emissions. At part load and early operation the emission level was low. And at higher load the level of emissions was high.

Research work carried out by Hailin et al. (2004) on the oil combustion in a spark ignition hydrogen engine was established by examining the exhaust concentrations of CO

and CO₂ and the intake mixture flow rate. The research engine was widely used for the knock rating of fuels. The spark ignition cooperative fuel research engine was operated on pure hydrogen at a compression ratio of 7 and a spark timing of 15 deg crank angle BTDC. Results showed that the emissions gradually increased as the equivalence ratio increased and once knocking took place the concentration of CO₂ increased while CO remained constant indicating that there was a sudden increase in the intensity of combustion. As the compression ratio was increased under non-knocking conditions the equivalence ratio played a major role in the oil combustion rate while compression ratio did have much effect. And on the onset of knocking the higher the compression ratio, leaner the equivalence ratio, resulting in rapid increase in rates.

Shudo et al. (2003) carried out experiments on a constant volume combustion chamber and subjected it to the use of stratified charge produced by direct injection. It used as a technique to reduce the cooling loss fraction and for improving thermal efficiency in hydrogen-combustion engines. The stratified charge by direct injection into the lean mixture reduced the heat transfer from the burning gas to the combustion chamber and increased the apparent heat-release fraction in hydrogen combustion. The degree of stratifications and the overall excess-air ratio achieved quite low-cooling loss fractions. As there was a reduction in the cooling loss fraction this led to a lower temperature of burned gas around the combustion chamber wall by the leaner mixture there formed by the stratification. It proved that the direct injection stratified charge, reduced the cooling loss fraction, thereby improving the thermal efficiency in hydrogen-combustion engines.

Work carried out by Robert et al. (2003) improved the performance of 2.0 L Zetec engine. Results showed that the performance of a gasoline engine with similar displacement could be matched or exceeded with hydrogen injection. Running with a super charger, air-to-air cooler, equivalence ratio fixed lean at a $\phi=0.5$ resulted in a torque deficit of 28% compared to gasoline. Thus supercharging, enriching the fuel-air mixture and utilizing an air-to-air intercooler reduced the torque to 7%. Furthermore, the experiments carried out using exhaust gas recirculation and three-way catalytic converter proved an effective means to reduce NO_x emissions to less than 1 ppm.

General Conclusions from Literature Review

- 1) Running the engine at $\phi < 0.6$ not only gave high thermal efficiency, high power output but also low NO_x emissions accompanied by high C.R of 10-12.
- 2) The power output of an engine running with hydrogen will be maximum if more air and hydrogen flow through it. Quality regulation gives higher thermal efficiencies rather than quantity regulation. The best performance of an engine can be obtained with injections quite before TDC.
- 3) Higher compression ratio's of over 13 can be used if the onset of pre-ignition is avoided.
- 4) NO_x emissions gradually increase as the equivalence ratio increase but on the other hand using lean air fuel ratio will generally decrease them.
- 5) A reduction in the cooling loss was essential for improving the thermal efficiency of hydrogen-fuelled engines.

CHAPTER 2

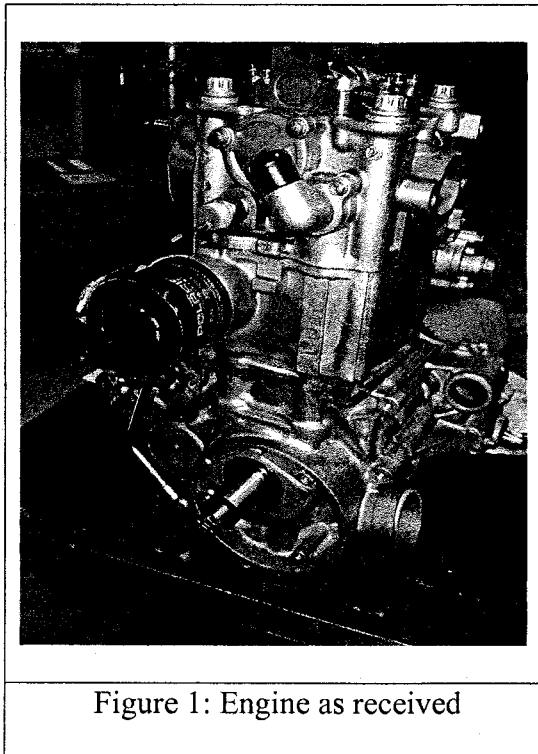
PHYSICAL DETAILS

The Polaris 2004 2x4 model, 425 cc four stroke single cylinder engine with a compression ratio of 9.2:1, has generally been designed for running on gasoline was received at University of Nevada, Las Vegas in the spring semester 2005. It has the rated power of 25 hp at 4000 rpm.

The engine was received without any throttle body connected to the intake manifold, no catalytic converter connected to the exhaust manifold, or any sensors hooked up. It was a raw engine for which some necessary parts had to be machined out at CNC in Kell's automotive, some sensors hooked up so as to bring the engine to baseline testing.

To run the baseline testing, one had to design the throttle body for the intake manifold so that the fuel injector could be incorporated. The idea was also to decrease the emissions for which a three way catalytic converter is attached to the exhaust manifold.

Figure 1 is a general picture of the raw engine as received.



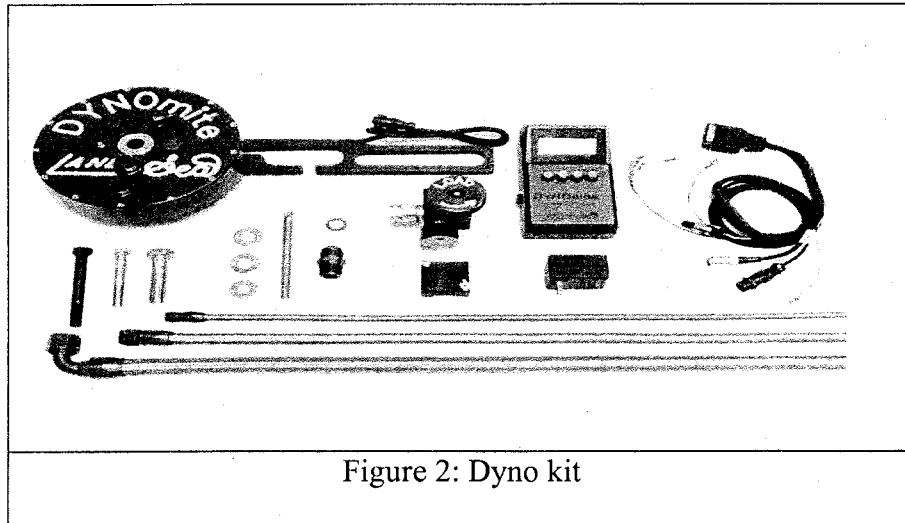
In order to test the Polaris engine, various testing equipment has been purchased from various dealers. The description of which are given below.

Testing Equipment

Dynamometer

The engine has been mounted directly with Land & Sea dyno which measures true horse power. The dynamometer computer records true horsepower, torque, rpm, elapsed time, etc while automatically applying inertia compensation and SAE correction factors for air temperature, barometric pressure, and relative humidity. Results display on the dynamometer's LCD and can be printed to an optional portable ASCII printer. It even doubles as a highly advanced on-sled racing data recorder. A standard dyno kit included

a 9 inch toroidal flow water brake absorber, an electronic torque arm transducer, engine load control, dynamite data acquisition computer with LCD and keypad interface option, AC power supply or re-charger, stainless braided hoses, data wiring harness, and protective carrying case. Figure 2 is a picture showing the dyno kit.



Dyno-max 2000™ software option creates a full engine dynamometer lab console on any PC. The features included real time trace graph display, EGT bar graph, inertia compensation, adjustable voice and visual limit-warnings, push button controls, and user configurable analog and digital gauge ranges. Data, reports, and publication quality graphs can be printed for customers-in full color. Figure 3 is a view of the software.

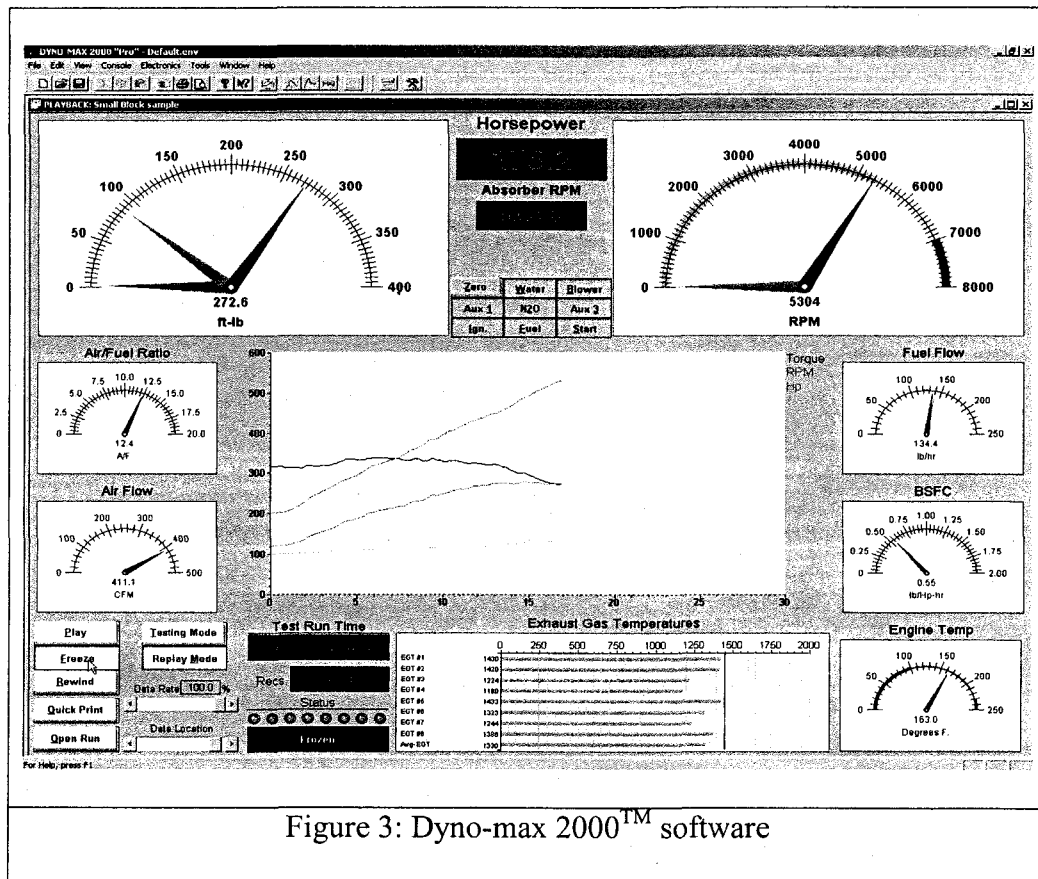


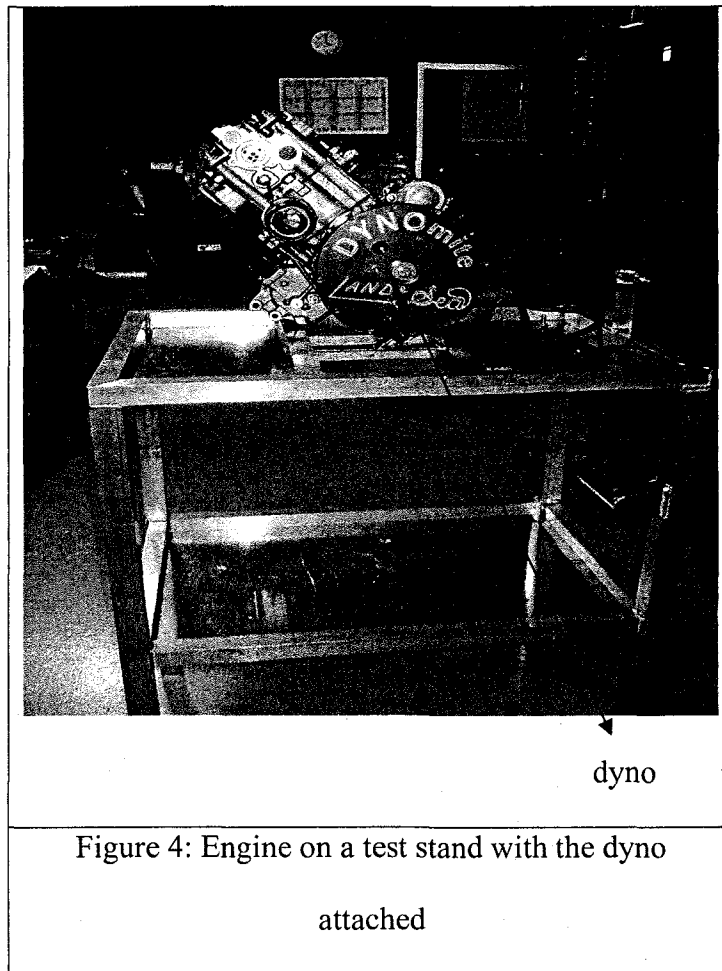
Figure 3: Dyno-max 2000™ software

Working of the Dynamometer

The dynamometer is a water absorption brake which receives inlet supply water via its load control valve assembly which it then pumps through specially designed recirculating torodial flow vanes. The test engine powers this “pump”. So, horsepower which is normally absorbed overcoming the drag and inertia of moving a vehicle is instead absorbed in the process of pumping the water through the brake.

The inertia and drag of the water continually accelerating and decelerating, as it circulates from the rotating impeller’s pockets to the stationary vaned stator pockets inside the absorber’s housing tries to rotate the entire absorber assembly. However a

torque arm attached to the stator housing prevents this rotation. Instead the forces acting on this torque arm bends it slightly in direct proportion to the applied torque. Figure 4 is a picture of the engine on a test stand with the dynamometer.



In order to maintain correct ignition and fuel injection timing of the engine a crank shaft sensor was attached to it. The hall-effect sensor is similar to a magnetic pulse unit in that it uses a stationary unit and a rotating trigger wheel. For this application the

magnetic pickup was chosen for the simplicity and easy implementation into the control unit. In order that we are able to attach this sensor to the engine, several brackets needed to be designed and manufactured. Figure 5 is a Solid Works representation of the brackets used.

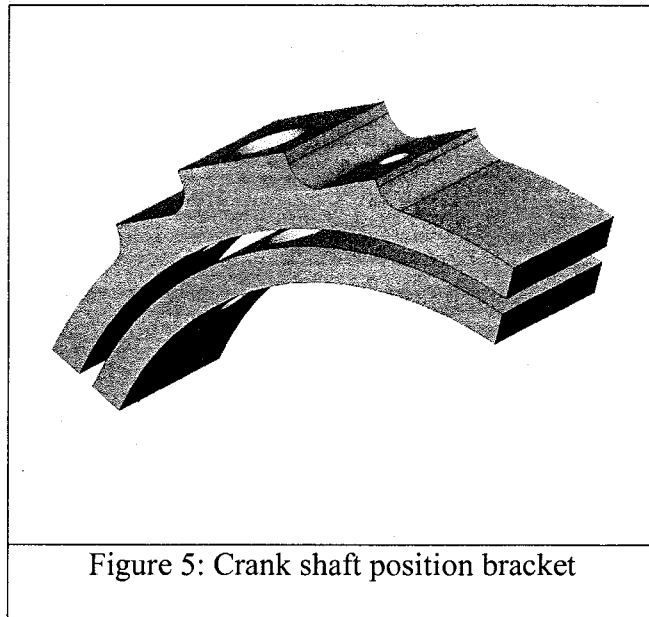
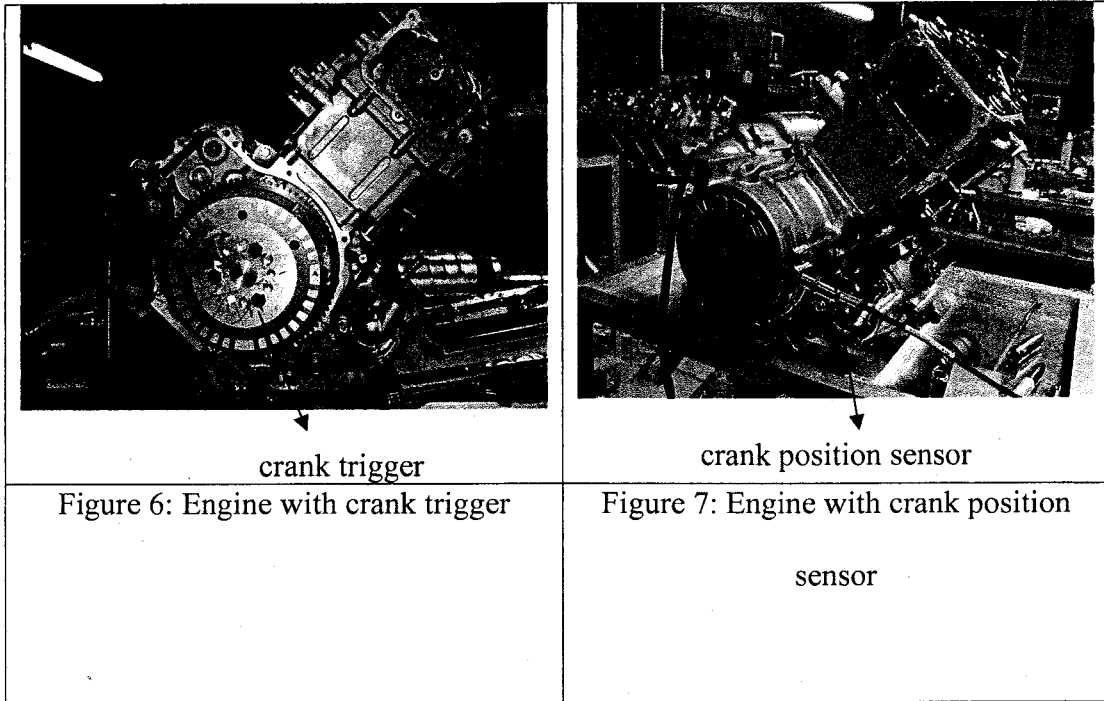
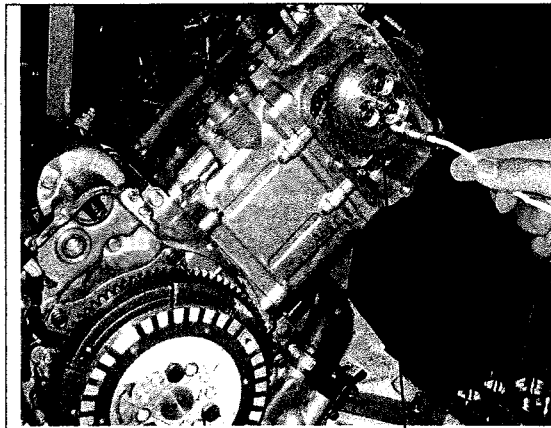


Figure 6 is the manufactured trigger wheel and Figure 7 is the crank position sensor installed on the motor.



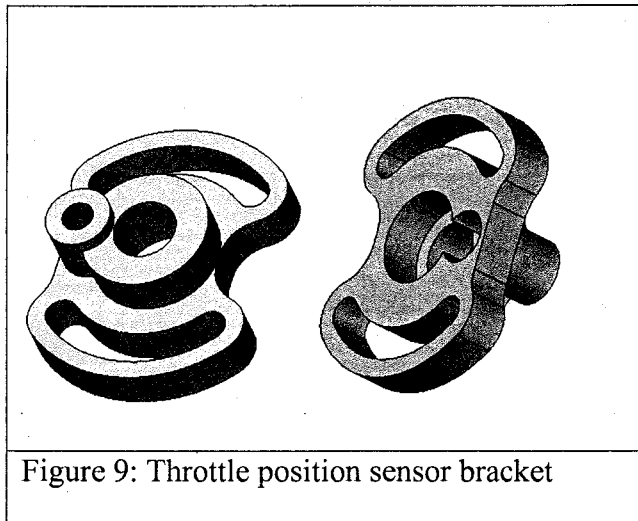
The engine was attached with a cam sensor so as to determine the exact point that the piston is at 'top dead center' for the compression stroke. This sensor was required for the computer system to track the valve operation. The engine would work without it, however, the spark would be initiated at both the compression and exhaust stroke. Figure 8 is a picture showing the cam shaft sensor.



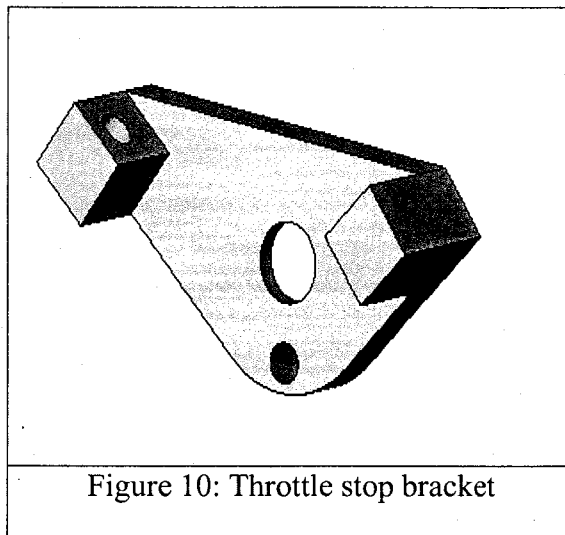
cam shaft sensor

Figure 8: Engine with cam shaft sensor

The engine was hooked up with a throttle valve position sensor to indicate the position of the throttle valve. It is usually mounted on the throttle body and converts the throttle valve angle into an electrical signal. As the throttle opens, the signal voltage increases. The following Solid Works diagram represents the bracket designed to mount the throttle position sensor to the new intake manifold. The main function of this sensor is to determine the exact position of the butterfly valve for the computer system.



Throttle stop bracket in Figure 10 was designed to protect the throttle position sensor from excessive angle as well as to set the idle.

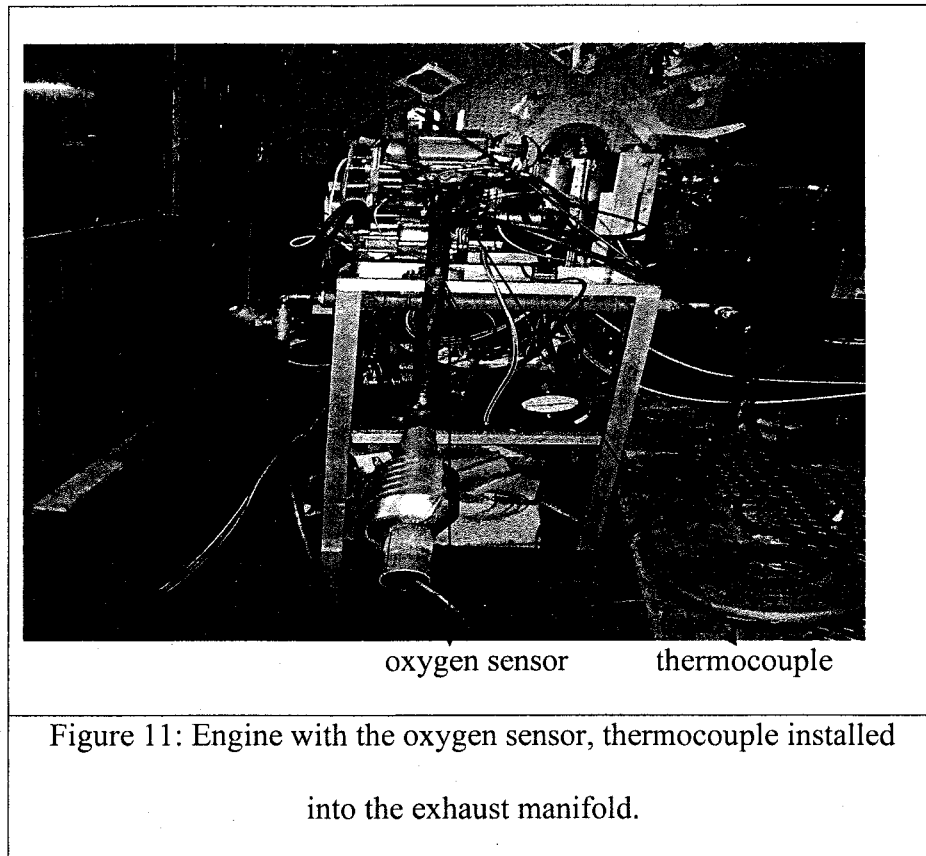


Engine was attached with a MAP and it refers to manifold absolute pressure sensor, a variable resistor used to monitor the difference in pressure between the intake manifold at outside atmosphere. This information is used by the engine computer to monitor engine load (vacuum drops when the engine is under load or at wide open throttle). When the engine is under load, the computer may alter spark timing and the fuel mixture to improve performance and emissions.

The air-fuel ratio of the engine was determined by attaching an oxygen sensor to the exhaust tail pipe. It is an advanced engine management (AEM) wideband oxygen sensor which detects the air-fuel mixture of the engine by measuring the amount of oxygen in the exhaust gas. The system consists of the AEM UEGO controller with wiring harness and one or two Bosch wide range sensors. The controller is available as both a single or dual channel system with one UEGO sensor per channel. Each oxygen channel features two different analog outputs, a 0-5 volt supply and 0-1 volt supply. The 0-1 volt is a lean to rich calibration specially designed to simulate the output range of a narrow band type sensor. The oxygen sensor rely on Nernst cell technology commonly called "Narrow Band", "2 wire" and sometimes erroneously described as "wide band". This is a cost effective method that outputs a voltage based on the oxygen content of the gas being sampled. It is accurate in the region surrounding stoichiometric operation and leaner. Unfortunately, in the rich region where high performance engines usually operate, their accuracy and repeatability is virtually non-existent.

The fuel-injection system will trim the mixture richer or leaner based on the signal from the oxygen sensor. It has been installed in the exhaust manifold, where the hot

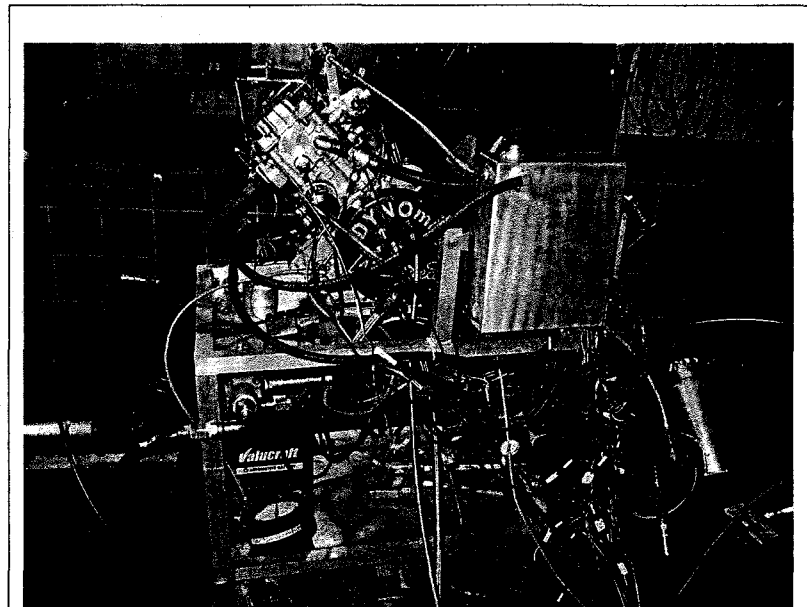
exhaust gases will pass by it. High temperature ($>350\text{ C}$) is required for the sensor to operate.



The engine has been installed with a thermocouple in the exhaust manifold in order to sense the exhaust gas temperature. It is a k-type thermocouple. Figure 11 shows the thermocouple.

The engine has been hooked up with an E-TEMP (Thermistor A) input lead which connects to a precision temperature thermistor for engine, oil or air temperatures up to 225 F.

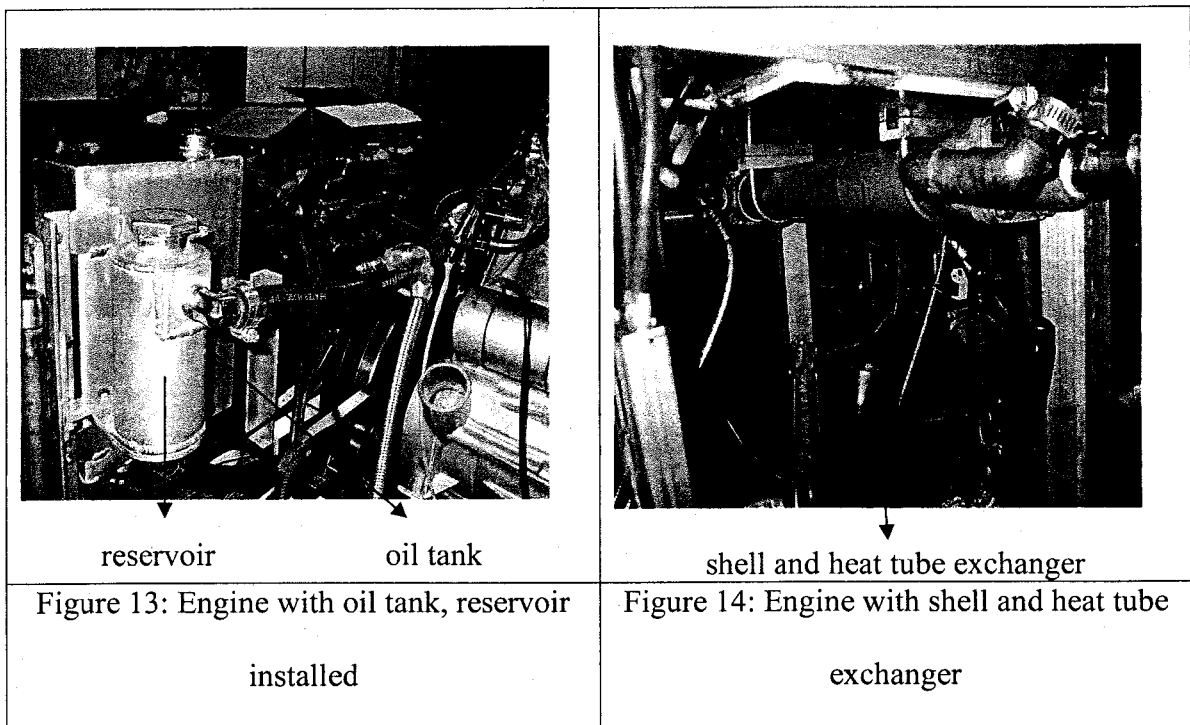
An engine coolant temperature sensor (ECT) has been located in the coolant passage just before the thermostat. It responds to change in engine coolant temperature. By measuring engine coolant temperature, engine control unit knows the average temperature of the engine.



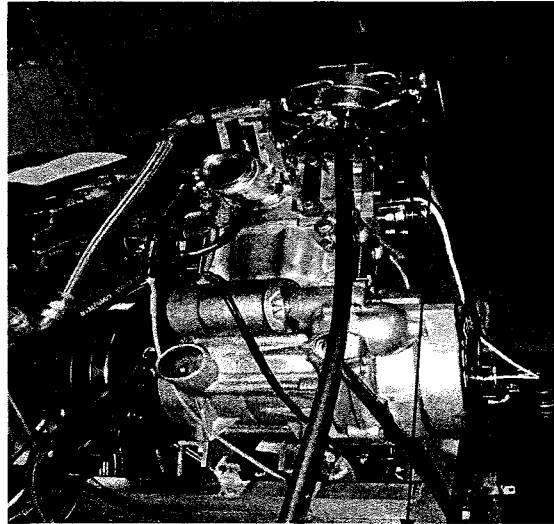
ECT
Figure 12: Engine with thermistor, engine coolant temperature sensor (ECT) installed

In order to provide the necessary oil to the engine crank case an oil tank has been attached at the appropriate position on the stand, as seen in figure12.

To provide a more reliable and permanent method of cooling for the engine which closely resembled the cooling system already utilized on the vehicle, a closed-loop water reservoir system was designed. This system consisted of manufacturing a reservoir and installing a shell and tube heat exchanger and they are shown in the figure 13 and figure 14.



The ignition system of the engine uses a spark plug which is energized by a super conducting wire. Figure 15 of the engine with the ignition coil (blue in color).

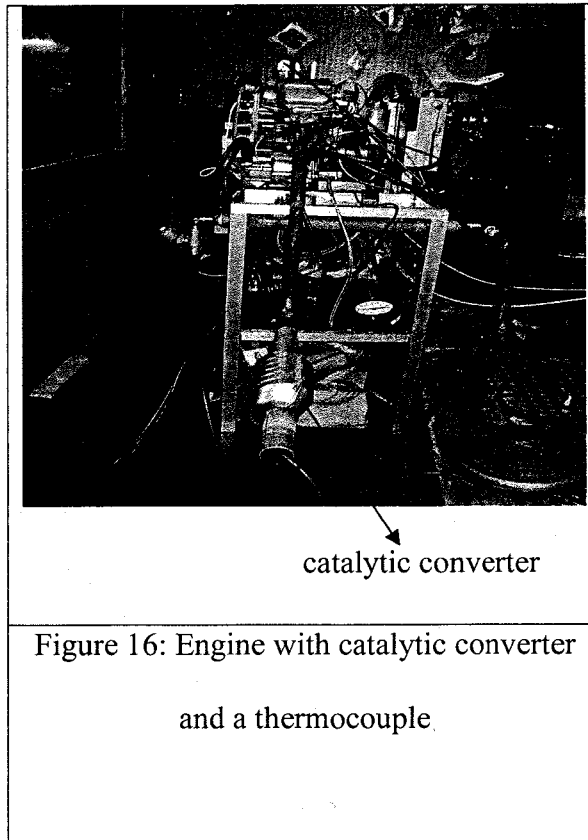


ignition coil

Figure 15: Engine with the ignition coil

(blue in color)

A three way catalytic converter has been attached to the exhaust manifold of the engine with the main intention of lowering the emissions. Figure 16 shows the catalytic converter.



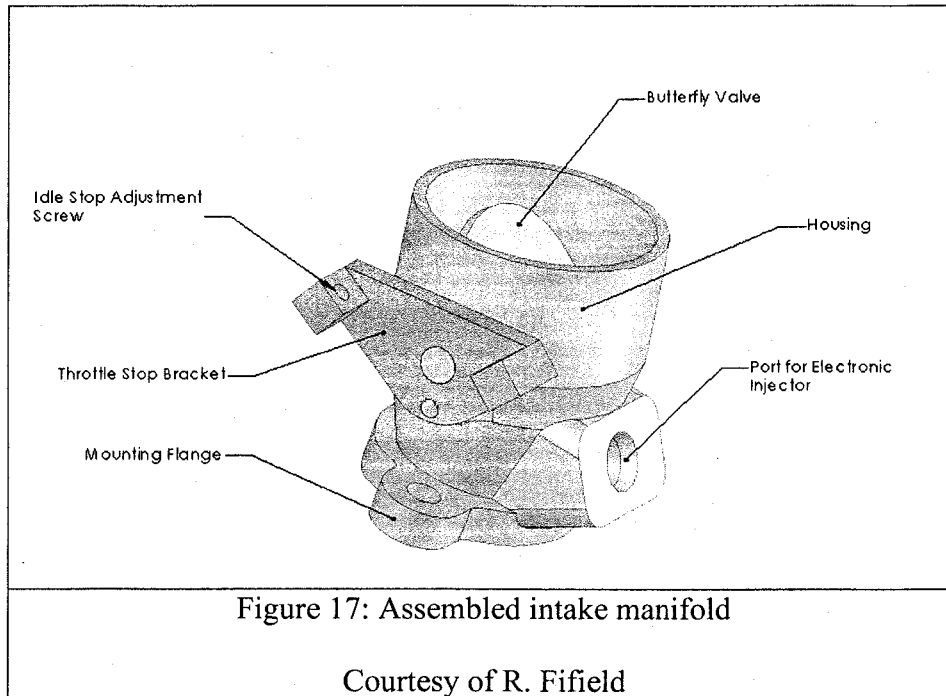
The emissions are measured using ECOM-AC which is a portable, microprocessor controlled, electrochemical sensor based emission analyzer that incorporates proven technology for accurate exhaust gas analysis. It provides measurements for O₂, CO (high range 0-40,000 ppm), NO, NO₂, SO₂ and hydrocarbons/combustibles.

Engine and its modifications.

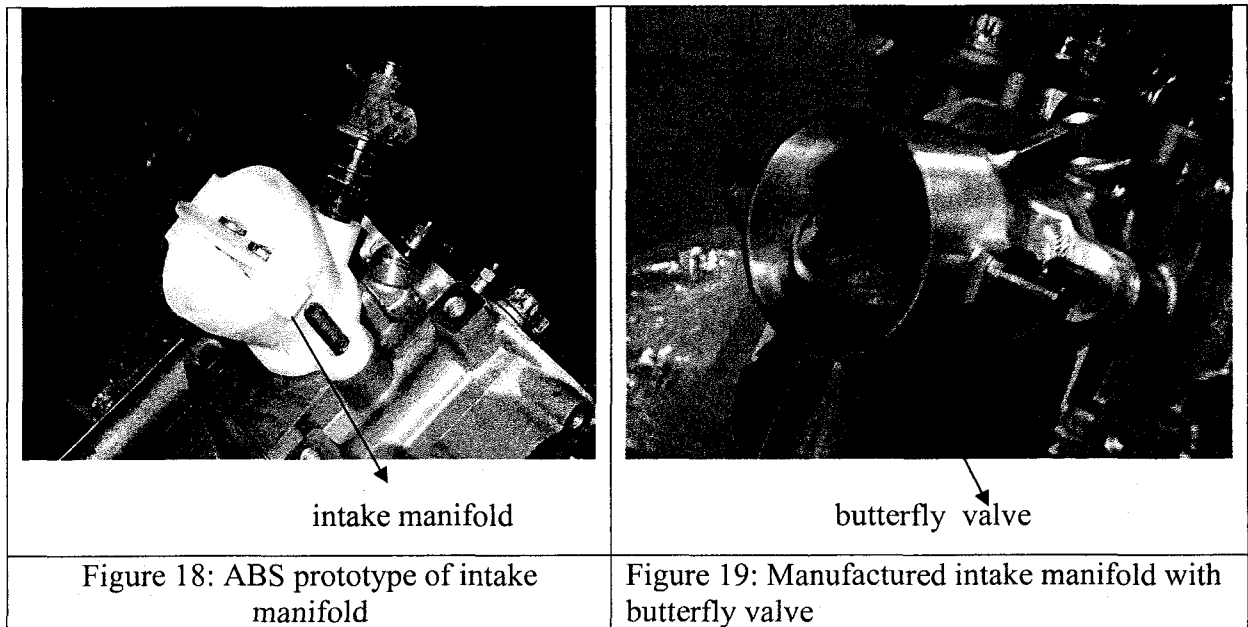
Modifications on the engine to run on gasoline

A newly designed intake manifold was fabricated out of aluminum using a CNC machine. Figure 17 is a Solid Works mock up. The main characteristics are a new port

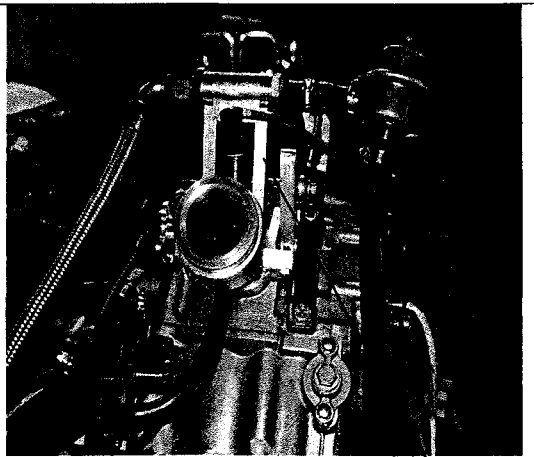
for an electronic injector used in setting the baseline parameters, attached throttle stop, butterfly valve, and the throttle position sensor not shown-on reverse side of manifold.



After the Solid Works rendering was complete, a prototype was constructed out of ABS plastic for mock-up purpose. Once all modifications were complete, the actual manifold was then fabricated out of aluminum using a CNC machine.



The intake manifold with the electronic fuel injector, a pressure regulator are connected to each other as shown below. Figure 20 shows the engine connected with throttle position sensor and also a map sensor.

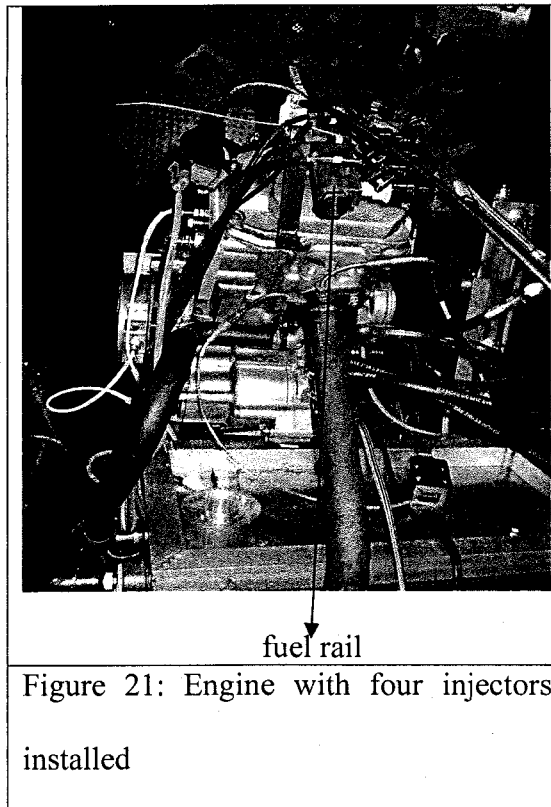


fuel injector

Figure 20: Manufactured intake manifold with the fuel injector

Engine as modified to operate on natural gas

Engine had the same sensors hooked to it but the supply of fuel switched to natural gas with four injectors attached to it. A fuel rail as seen in the figure 21 was fabricated out of aluminum using a CNC machine in-order to incorporate the injectors.



Engine as modified to run on port injection of hydrogen

Port Injection

Research was conducted for a hydrogen injector in the market and then we found an Austrian company which would supply the Hoerbiger injector to UNLV. But there was a research delay because it was misplaced for around 3 months. After it arrived, it was installed with a new throttle body design not with many modifications. It worked for 4-5 hours of operation accompanied with a lot of back fire, pre-ignition and knocking. But stopped later due to fatigue and vibration problems pertaining to the injector. Three main problems occurred due to vibration. The dowel pin which aligns the inlet boss to the electro-magnet sheared. This caused the second problem. When the pin sheared, the two

components (inlet boss and coil) were allowed to rotate in opposite directions thus causing the o-rings that seal the wires to the inlet boss to deform and leak. The third problem was the locknut for the inlet boss (originally lock-tighted) backed off causing the air gap between the electro-magnet/coil and the inertia plate to be too.

We could not record much data while it was running because the engine could not be tuned to run smoothly, taking into account the time factor of operation of only 4-5 hours.

Figure 22 is a picture of the engine with Hoerbiger injector.

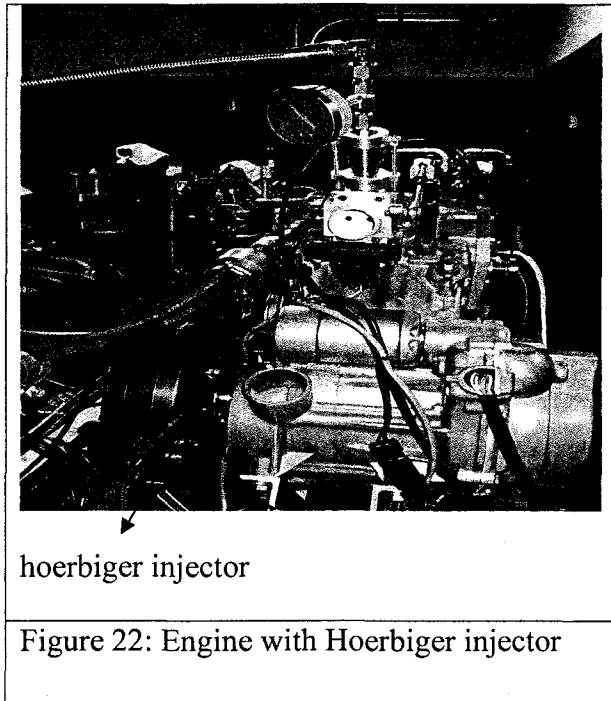
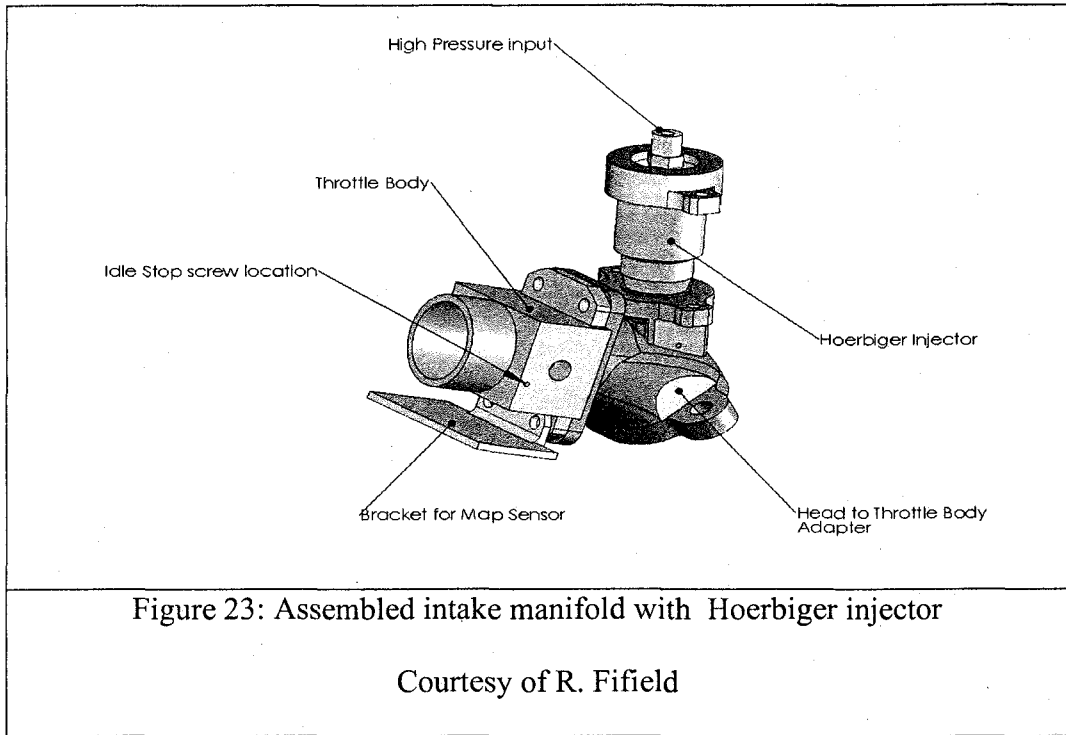
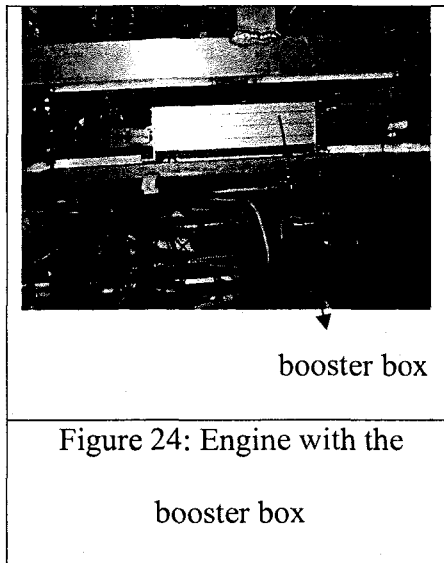


Figure 23 is a Solid Works representation of the Hoerbiger injector with the throttle body design.



The injector timing was controlled by another computer known as the booster box provided by Hoerbiger. It is shown in the figure 24.



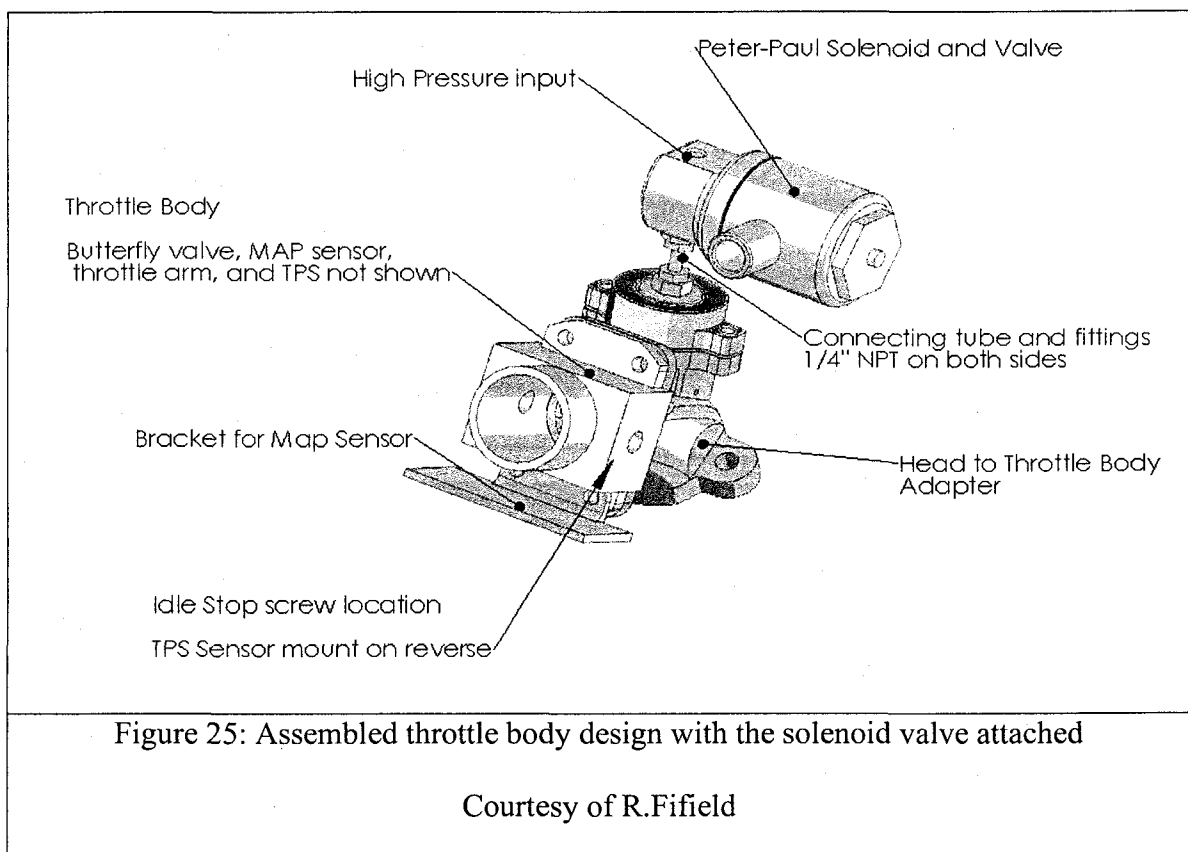
The booster box is used to control the Hoerbiger injector which is normally fed with power whenever the ignition key is on. The booster box controls the negative, or ground side, of the circuit. When the computer provides the Hoerbiger injector with a ground, the circuit is completed and current is allowed to flow through it. This energizes an electromagnetic coil inside the Hoerbiger injector, which pulls a sealing mechanism (pintle, ball, or disc) away from its seat. This makes it possible for fuel to flow through the injector and into the engine. When the computer removes the electrical ground to the injector, the electromagnetic coil becomes demagnetized and a spring forces the pintle, ball, or disc shut to cut off fuel flow.

The booster box is used to control the response time of the high pressure Hoerbiger injector. Due to the limitations of the controller in the primary computer (total internal resistance of 1000Ω is allowable through the injector), a booster box is used in conjunction with the primary computer to boost the voltage supply to the injector for a specified time thereby decreasing the response time for the injector to open.

A second approach was planned, for in-cylinder fuel injection using a two way normally closed high pressure impact type solenoid valve purchased from Peter Paul. The solenoid valve is simple in construction with only two moving parts. Its exclusive features include a precision stainless steel plunger that supplies the necessary impact force to energize the valve, a Kel-F PIN functioning as a sealing element, that is carefully machined for maximum concentricity and fine finish, and a orifice guide for near perfect alignment, giving a bubble-tight sealing from low pressures right up to maximum pressure rating with the bonus of longer life.

Principles of operation of the solenoid valve

When the valve coil is energized, the plunger is drawn towards the sleeve end stop. The plunger is allowed to accelerate freely for a short distance before it makes contact with the pin shoulder. Upon contact it imparts considerable force on the pin causing it to lift off the seat. A return spring provides the return force, directly on the pin, to seal the orifice when the coil is de-energized. It successfully ran with hydrogen but was also accompanied with pre-ignition, back-firing and knock. Figure 26 shows the basic Solid Works design of the solenoid valve with the throttle body assembly. The throttle body was then fabricated out of aluminum using a CNC machine.



Unfortunately, we were unmindful of taking the engine's picture with the solenoid valve. But in place of the Hoerbiger injector, we installed a solenoid valve and its timing was also controlled by the booster box provided by Hoerbiger. We were able to collect some data with it. The solenoid's pressure was controlled between 100-150 psi.

Initial tests consisted of operating the engine at 1500, 2000, 2500, and 3000 rpm with a load of 50%, 75%, and 100%. Results showed that at an air fuel ratio of 40:1, a power output of 2-3 was accompanied by frequent popping sound. So, we had to maintain the engine speed at 2000 rpm. But as the speed increased, it resulted in a decrease in the power of the engine because of pre-ignition of hydrogen, and the problem was rectified by adding more fuel and by increasing the water temperature. But the engine stopped after running at these greater water temperatures. The engine performance was low while comparing it to that obtained with gasoline and natural gas. This behavior was due to the larger flammability limits of hydrogen. Previous research by Guo et al. (1999) highlights the fact that abnormal combustion accompanied with small power output had been avoided when a high pressure hydrogen injector was designed to improve hydrogen jet penetration and mixture formation in the combustion chamber, and to prevent backfire occurring in the hydrogen supply pipe between the fast response solenoid valve, which had good switch characteristics, and the combustion chamber. The main advantage with their system was that, even at higher speeds, the solenoid valve had good switch characteristics and very fast response.

The disadvantage of running the Polaris Ranger engine with port injection of hydrogen was that we could not properly tune the engine at higher speeds with the solenoid valve from Peter Paul. The problem of pre-ignition, back-fire and knock,

persisted, and after reaching higher temperatures the engine abruptly stopped. After running the engine again, it would start but after reaching high temperatures, it again stopped.

The levels of NO_x emissions were low in the range of 1000-4000 ppm, and at an air fuel ratio of 40:1. The levels of CO were very low ranging from 100-300 ppm, it was found these were low when compared to the figures obtained from gasoline or natural gas. We assume that this abnormal behavior of CO levels might be due to the impurities present in the hydrogen gas, or due to the oil combustion.

Direct injection of hydrogen

The head was modified by drilling a hole in such a way so as to incorporate the second Hoerbiger injector. When unstable, lasted only for 25 minutes and finally started to leak as the same problem of vibration persisted. We were unsuccessful the second time too and couldn't get any data.

Initial testing of the Hoerbiger injector consisted of flowing it on air at a 75% cycle duty for approximately 25 minutes. No leak was detected and full control over flow was noted. Second flow test consisted of operating the injector on hydrogen at a 90% cycle duty. The results from this test were inputted into ECM as a max flow capacity.

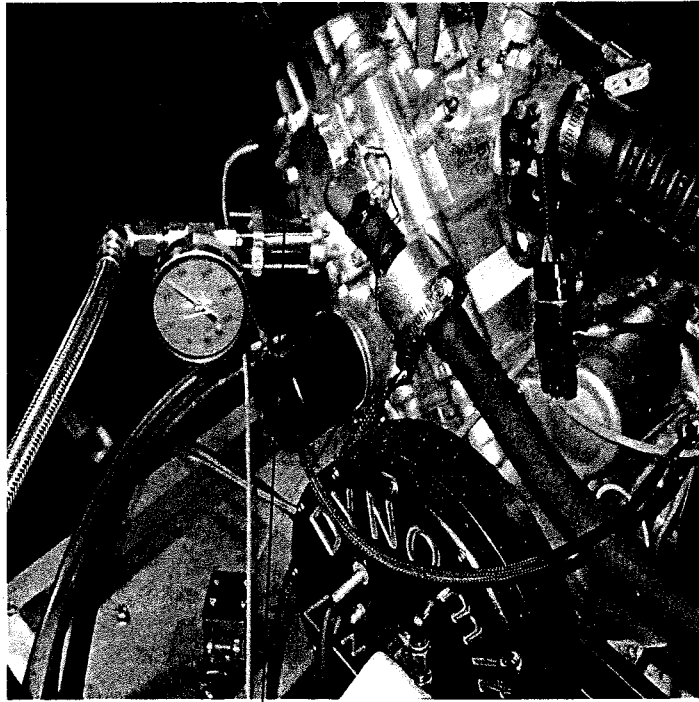
Testing plans for injector, installed in the engine, consisted of operating the engine at 1500, 2000, 2500, and 3000 rpm with a load of 50%, 75%, and 100%. Approximately 5 minutes into test, at 2000 rpm and 75% of max load, the response of the motor became sluggish. Less than a minute later the engine abruptly stopped. In subsequent attempts to restart close attention was given to the mass flow meter to verify adequate fuel was

delivered during startup. It was noted that an unusually high amount of fuel was being delivered. Upon further inspection it was also noticed that flow through the injector never ceased regardless of whether or not the solenoid was energized. Upon removal of the injector from the engine, it was confirmed that gas continued to flow (power turned off). After reviewing the data collected from the ECM, it was also verified that then engine became extremely rich (air fuel ratio of 5:1) seconds prior to shutting off.

Pre-installation flow results: 3.6 lb/hr H₂ (90% cycle duty).

Post failure flow results: 2.5 lb/hr H₂ (Unenergized), 3.8 lb/hr H₂ (90% cycle duty).

The possible reason for failure, based on previous failure on different injector of the same type and manufacture, is fracture of main seal. Failure did not hinder operation of solenoid as it was reactive. This type of failure was further confirmed by an increase in flow, a direct result of the seal fracturing and thereby increasing the port size. Figure 27 depicts the engine with the second Hoerbiger injector.



hoerbiger injector

Figure 26: Engine with the second Hoerbiger injector

Figure 27 is a Solid Works representation of the engine with the in-cylinder hydrogen injection with Hoerbiger injector.

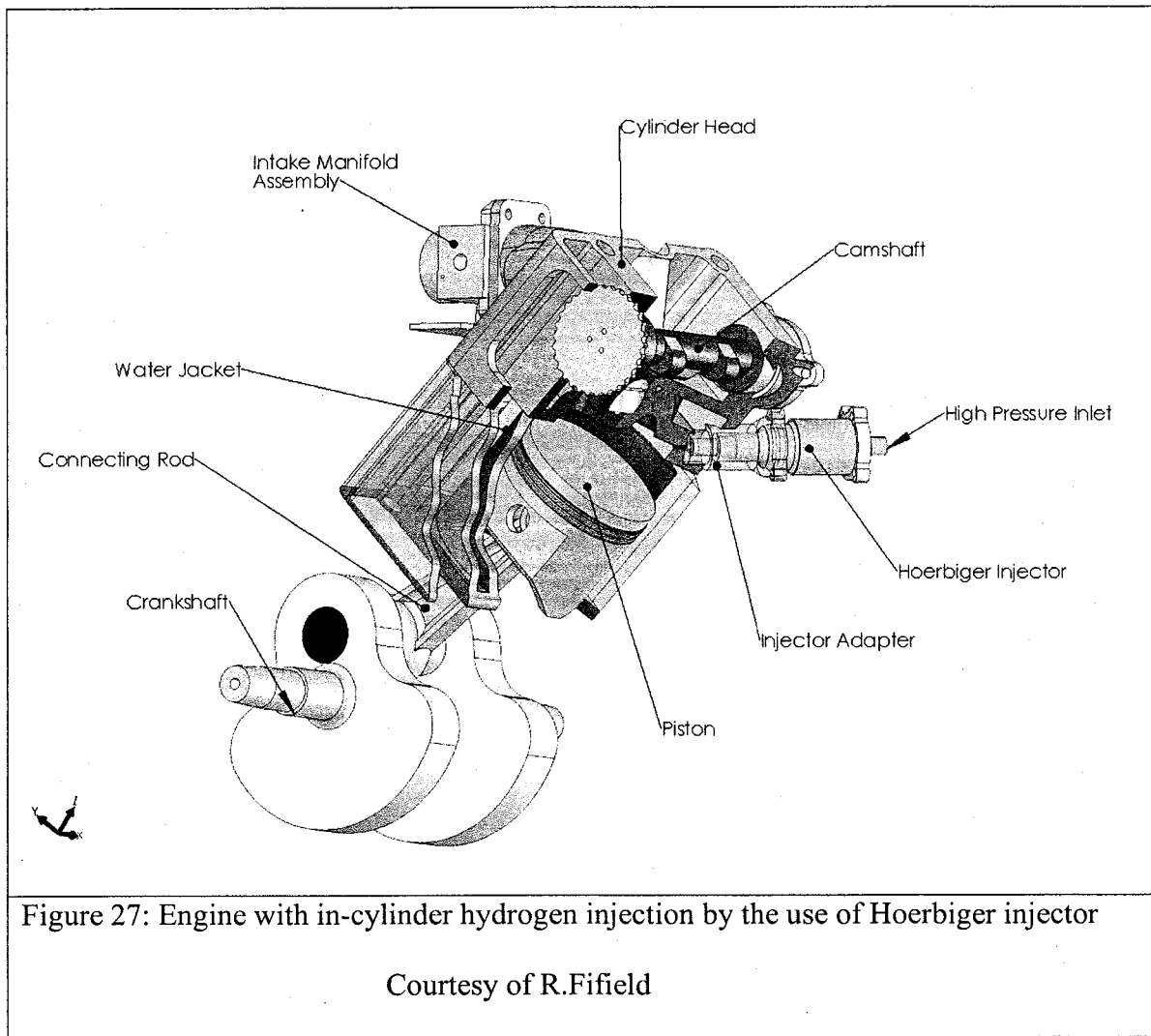


Figure 27: Engine with in-cylinder hydrogen injection by the use of Hoerbiger injector

Courtesy of R.Fifield

The engine's head was drilled in such a way so as to incorporate the Hoerbiger injector in an adapter. It was pressure tested for any leaks and found to be good.

We had a second approach of using the solenoid valve instead of the Hoerbiger injector. But after running the engine with in-cylinder injection, we had a false reading for the A/f ratio's because peak power was achieved at an a/f ratio of 20:1 to 25:1, however after a full test of the O₂ sensor was performed, it was determined that the sensor was working but out of required exhaust

temperature levels. In short, the O₂ sensor required a minimum exhaust temperature of 300 C or approximately 572 F of which we were unable to achieve at low loads or engine speeds. An appropriate O₂ sensor was installed. Secondly, a mass air fuel (MAF) sensor was also installed as a means to verify the new O₂. With the mass of the fuel and air known, the a/f ratio was calculated and subsequently verified with the O₂ sensor.

A mass flow meter was calibrated and fitted to the motor. Tests with the engine running indicate an ok difference between the new O₂ setup and the calculated air fuel ratio using mass air sensor and mass flow meters was less than 1.2 %. A new fuel map was programmed into the computer and initial runs indicated a peak horsepower of 11.5 achieved at an air fuel ratio of 32:1 slightly above stoichiometric.

The timing of the fuel was adjusted to slightly before top-dead center on the compression stroke by 300 to 350 deg after traditional injection. We believe that this method will help alleviate issues arising from the slow response in the solenoid and issues due to an abrupt increase in pressure during compression.

Finally, two mass flow meters were attached to the engine. Figure 29 shows both of them attached.

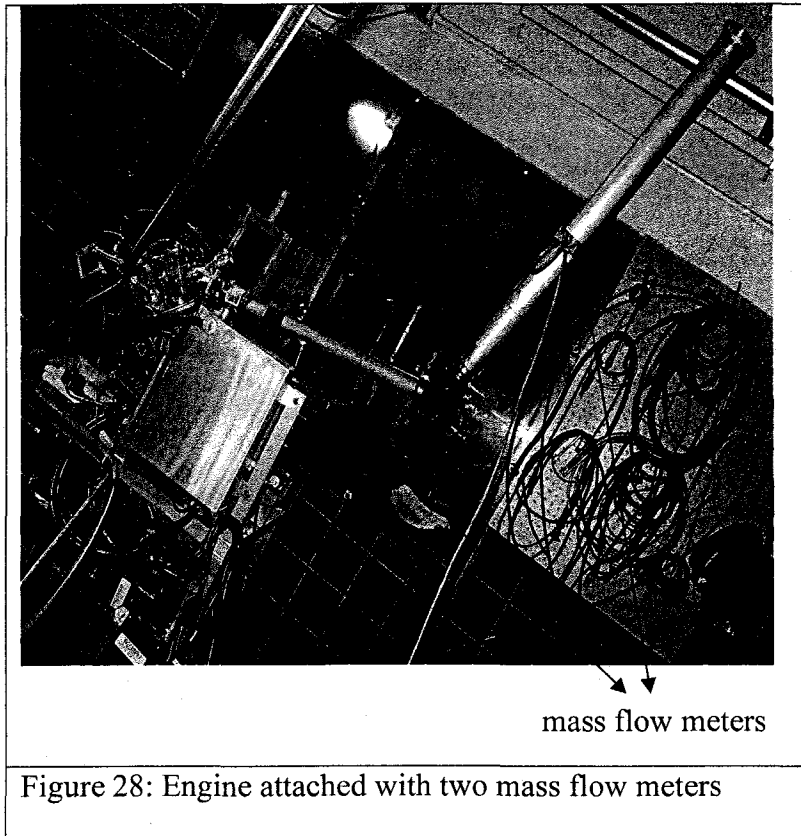
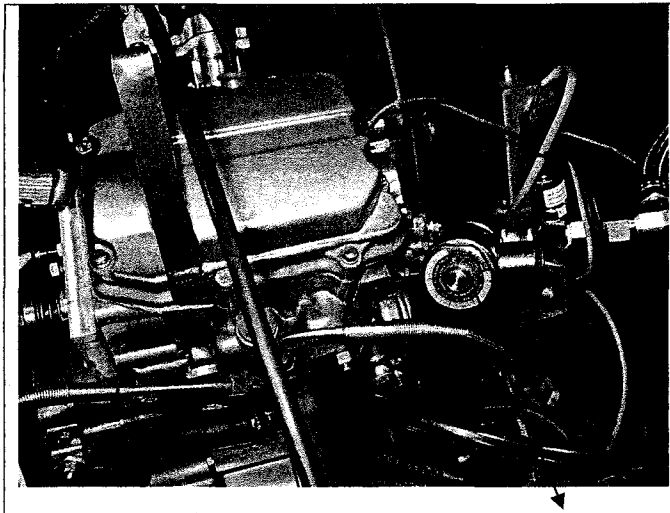


Figure 29 shows the engine with the solenoid valve attached.



solenoid valve

Figure 29: Engine with solenoid valve attached

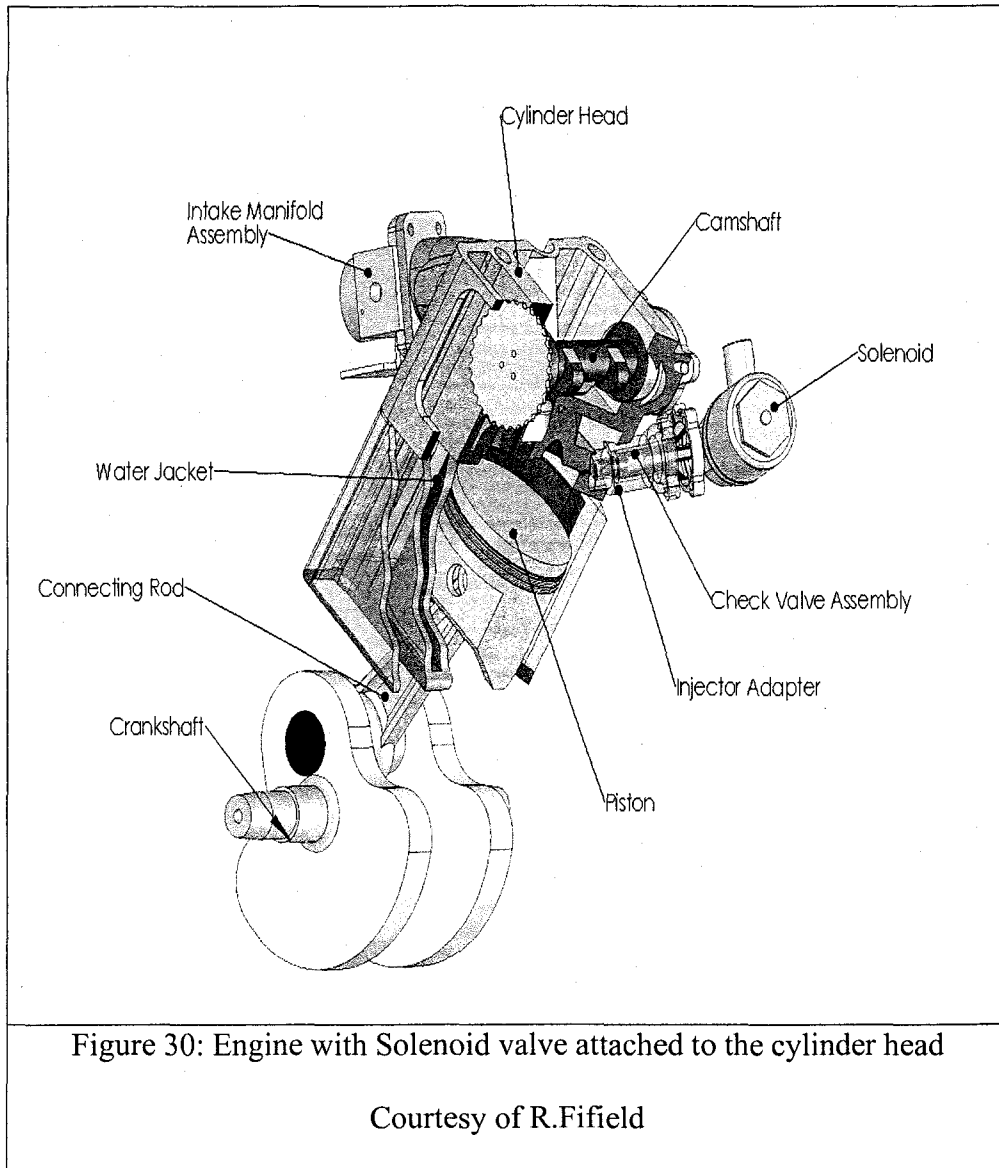
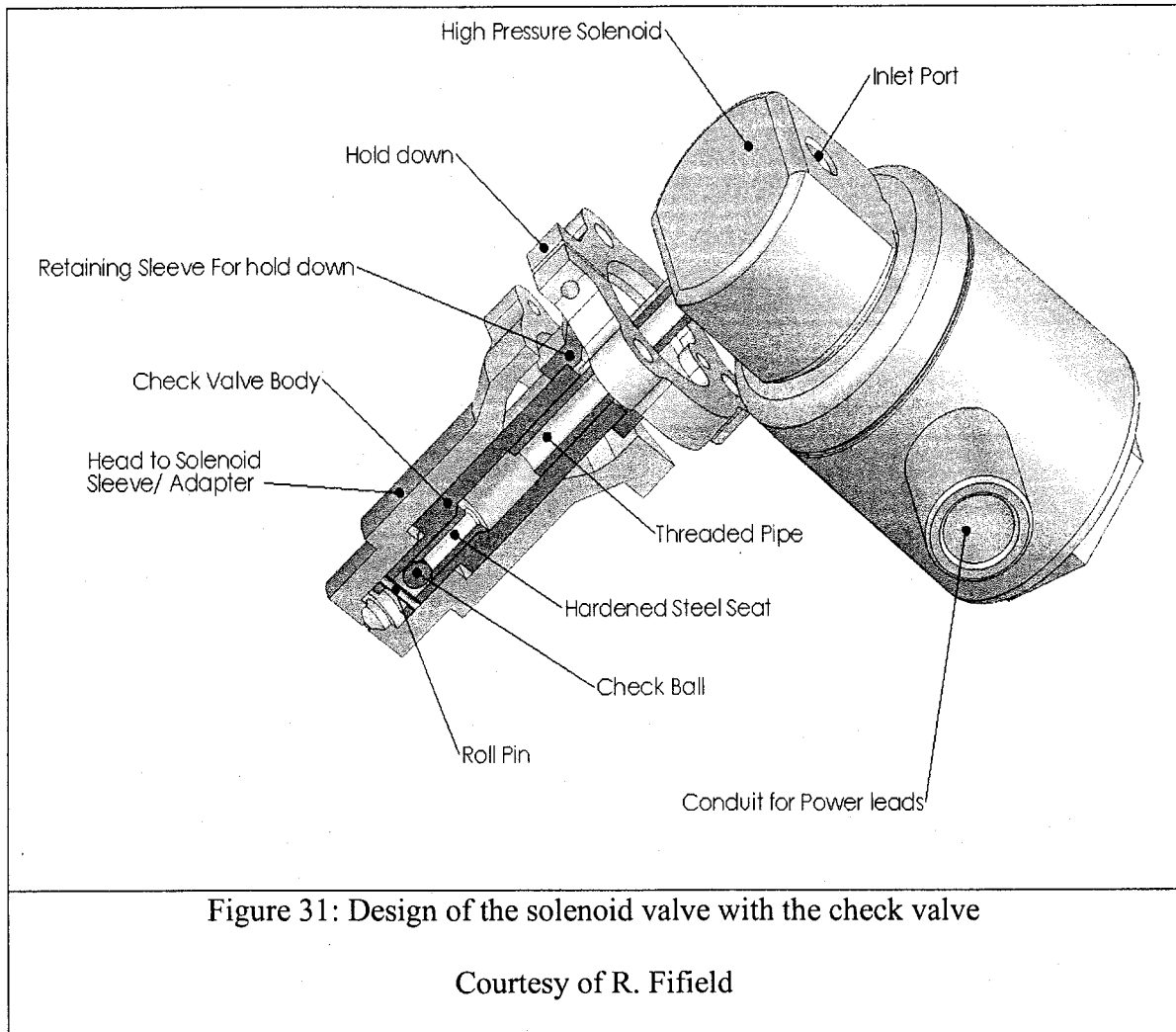


Figure 30 shows the solenoid valve connected to the engine head. In order to avoid the flow of hydrogen in the opposite direction, a check valve assembly was fabricated and connected to the solenoid valve. The hydrogen pressure was regulated between 150-300 psi by a high pressure regulator hooked up to the hydrogen tanks. The tanks contain

99% purity gas. The solenoid injection timing was controlled by the booster box provided along with the Hoerbiger injector.



Testing for the solenoid valve, installed on the engine, consisted of operating the engine at 1500, 2000, 2500, and 3000 RPM with a load of 50%, 75%, and 100%. Running at speeds of 2000 and 3000 rpm and at a calculated air fuel ratio of 20:6, we obtained a power of 3.5 and 7 hp respectively. The remarkable feature of running the

engine with in-cylinder injection of hydrogen proved to be good because we obtained zero NO_x emissions. We were unable to tune the engine beyond 3000 rpm, because the problem of pre-ignition persisted.

Further research has to be carried out on the Polaris Engine to get more comprehensive results. Finally, we were able to run the Polaris Ranger with in-cylinder injection of hydrogen and obtained a peak power of 11.5 hp at an air fuel ratio of 32:1 slightly above stoichiometric with zero NO_x emissions.

CHAPTER 3

PERFORMANCE AND EMISSIONS EVALUATION

After the baseline testing of the engine with gasoline, the performance was evaluated. Tests were carried out at different speeds, different air fuel ratios and at wide open throttle. The power and torque have been compared at these levels.

Engine performance while operating on gasoline

- 1) Comparison of observed torques at different speeds and different air fuel ratio's carried out at wide open throttle 28" Hg.

Table 1: Different torques at different speeds, A/F ratio's and WOT 28" Hg (gasoline) are shown

Rpm	Torque(1) (Nm)	Torque(2) (Nm)	Torque(3) (Nm)
2000	22	21	21
3000	24	22	22
4000	23	24	23

Where (1) represents an lean air fuel ratio of 13.7

(2) represents an stoichometric air fuel ratio of 14.7

(3) represents an rich air fuel ratio of 15.7

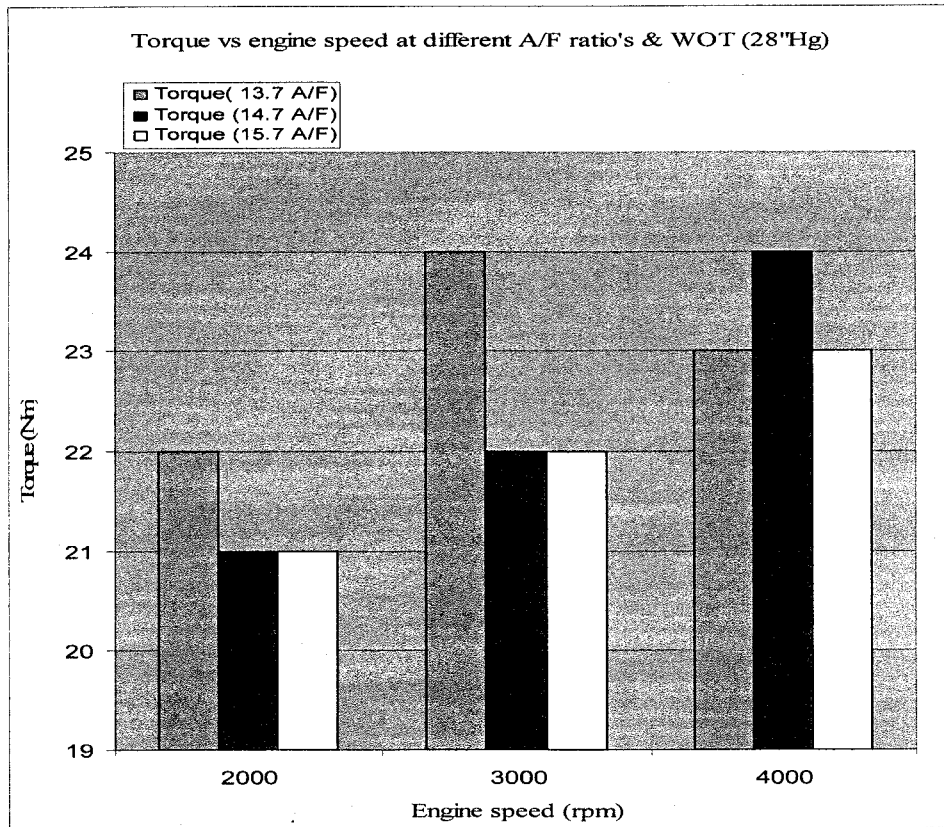


Figure 32: Comparison of torques at different speeds (gasoline)

The Society of Automotive Engineers (SAE) created a standard method for correcting horsepower and torque readings so that they will seem as if the readings had all been taken at the same "standard" test cell where the air pressure, humidity and air temperature are held constant.

The equation for the dyno correction factor given in SAE J1349 JUN90, converted to pressure in mb, is:

$$cf = 1.180 \cdot \left[\left(\frac{990}{P_d} \right) \cdot \left(\frac{T_c + 273}{298} \right)^{0.5} \right]^{-0.18}$$

where: cf = the dyno correction factor

P_d = the pressure of the dry air, mb

T_c = ambient temperature, deg C

The pressure of the dry air P_d , is found by subtracting the vapor pressure P_v from the actual air pressure. The relative horsepower is simply the mathematical reciprocal of the correction factor. On that particular date of test we obtained corresponding corrected values of torques varied from 59-29 (Nm) for the speeds varying from 2000-4000 rpm.

2) Comparison of power output at different speeds and different A/F ratio's carried out at wide open throttle 28" Hg.

Table 2: Power output at different speeds, A/F ratio's and WOT 28" Hg (gasoline) are shown

Rpm	HP(1)	HP(2)	HP(3)
2000	8.38	8.00	8.00
3000	13.71	12.57	12.57
4000	17.52	18.28	17.52

Where (1) represents an lean air fuel ratio of 13.7

(2) represents an stoichometric air fuel ratio of 14.7

(3) represents an rich air fuel ratio of 15.7

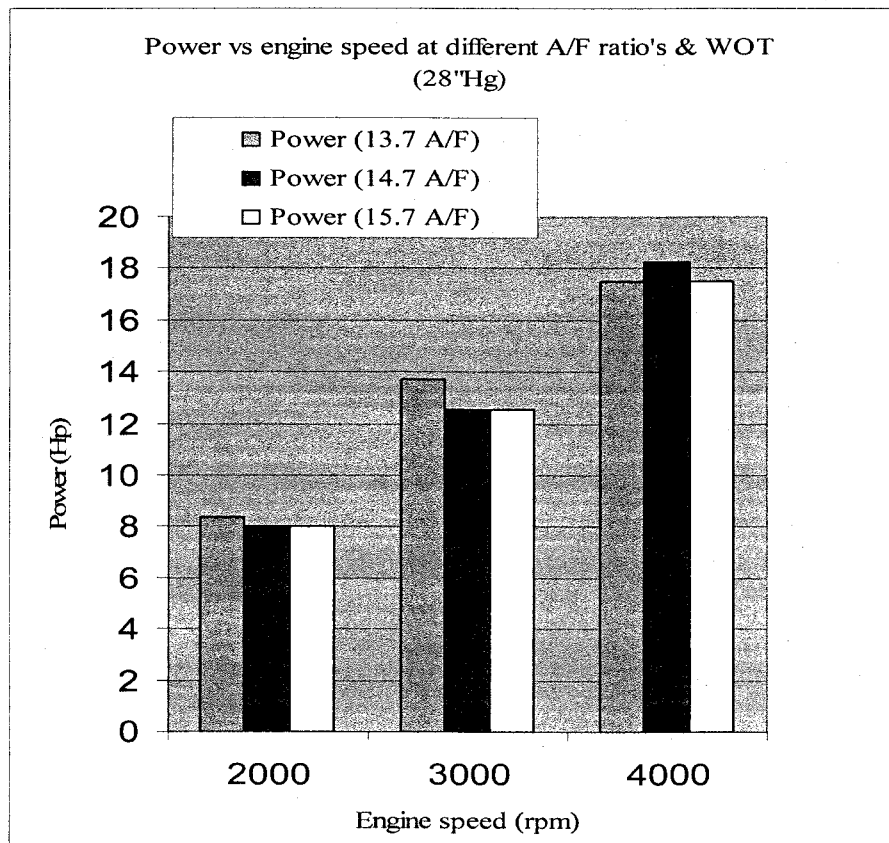


Figure 33: Comparison of power output at different speeds (gasoline)

The corresponding corrected values of power output gave a constant value of 22.468 hp for the speeds varying from 2000-4000 rpm.

Engine emission evaluation while operating on gasoline

- 1) Comparison of the emissions before and after a catalytic converter at different speeds and wide open throttle 28" Hg and at stoichiometric air fuel ratio 14.7.

Table 3: Emissions observed before and after catalyst at different speeds, WOT 28”Hg and 14.7 A/F ratio (gasoline) are shown.

Rpm	CO(B)	CO(A)	No _x (B)	No _x (A)
2000	4000	670	2900	217
3000	4000	3221	3000	450
4000	4000	4000	3000	555

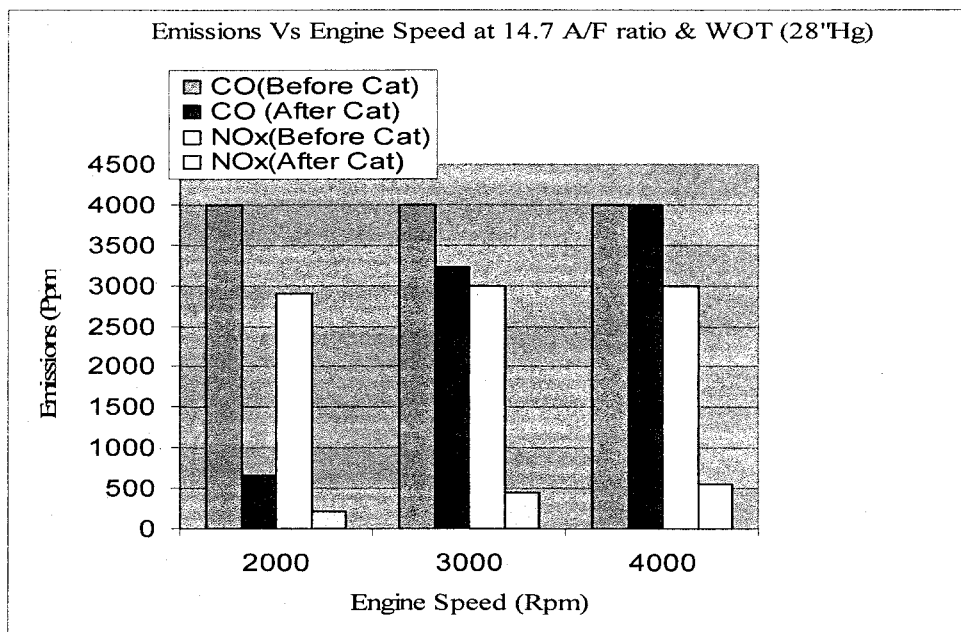


Figure 34: Comparison of emissions at different speeds and stoichiometric air fuel ratio (gasoline)

It can be inferred from the graph that the levels of CO and NO_x have considerably reduced after the catalytic converter but at times the levels of CO were unchanged. It seems to be an irregularity.

2) Comparison of the emissions before and after a catalytic converter at different speeds and wide open throttle 28”Hg and at lean air fuel ratio 13.7.

Table 4: Emissions observed before and after catalyst at different speeds, WOT 28" Hg and 13.7 A/F ratio (gasoline)

Rpm	CO(B)	CO(A)	No _x (B)	No _x (A)
2000	4000	4000	2040	424
3000	4000	4000	2050	510
4000	4000	4000	2155	744

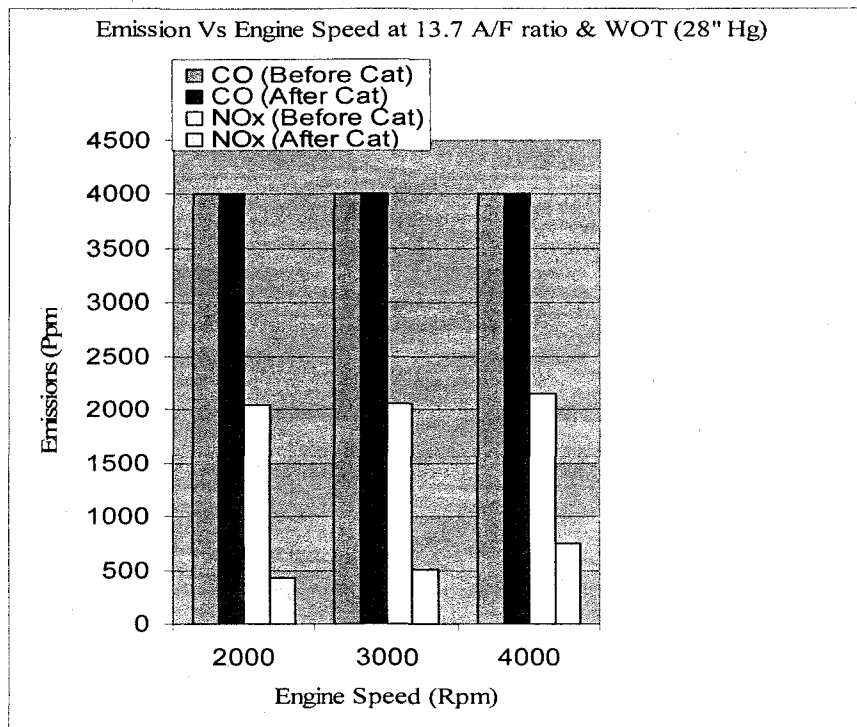


Figure 35: Comparison of emissions at different speeds and lean air fuel ratio 13.7 (gasoline)

3) Comparison of the emissions before and after a catalytic converter at different speeds and wide open throttle 28" Hg and at rich air fuel ratio of 15.7.

Table 5: Emissions observed before and after catalyst at different speeds, WOT 28" Hg and 15.7 A/F ratio (gasoline)

Rpm	CO(B)	CO(A)	No _x (B)	No _x (A)
2000	1600	120	4000	4000
3000	1550	145	3000	3000
4000	990	184	3700	3500

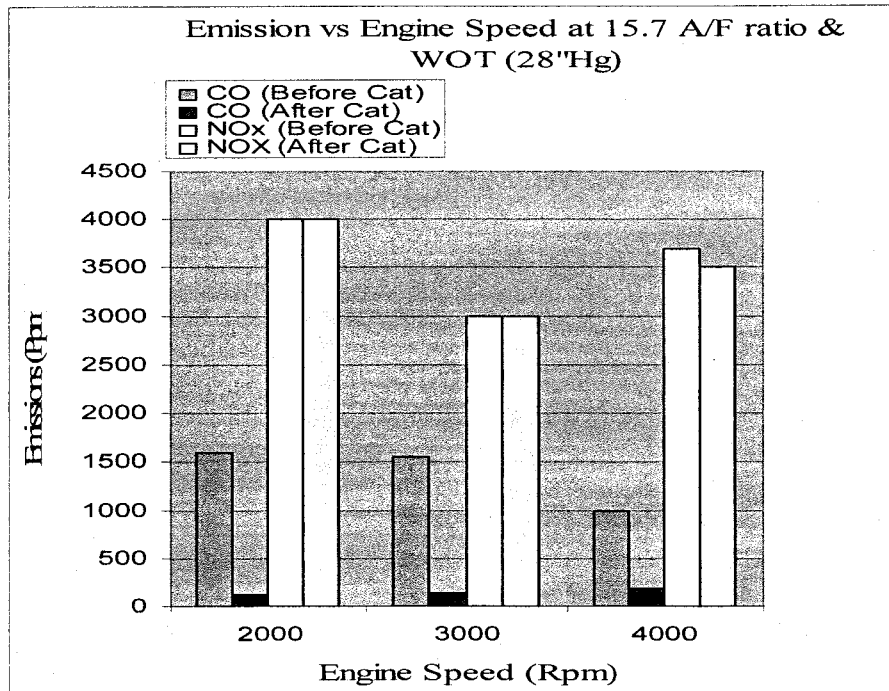


Figure 36: Comparison of emissions at different speeds, WOT 28" Hg and rich air fuel ratio 15.7 (gasoline)

The performance of the engine has been evaluated by comparison of torque and power at different speeds, different air fuel ratios and at wide open throttle.

Engine performance while operating it on natural gas

1) Comparison of torques at different speeds and different air fuel ratios carried out at wide open throttle 28”Hg.

Table 6: Different torques at different speeds, at different A/F ratio's and WOT (natural gas)

Rpm	Torque(1) (Nm)	Torque(2) (Nm)	Torque(3) (Nm)
2000	18	18	16
3000	18	18	18
4000	18	19	18

Where (1) represents an lean air fuel ratio of 14

(2) represents an stoichometric air fuel ratio of 14.5

(3) represents an rich air fuel ratio of 15

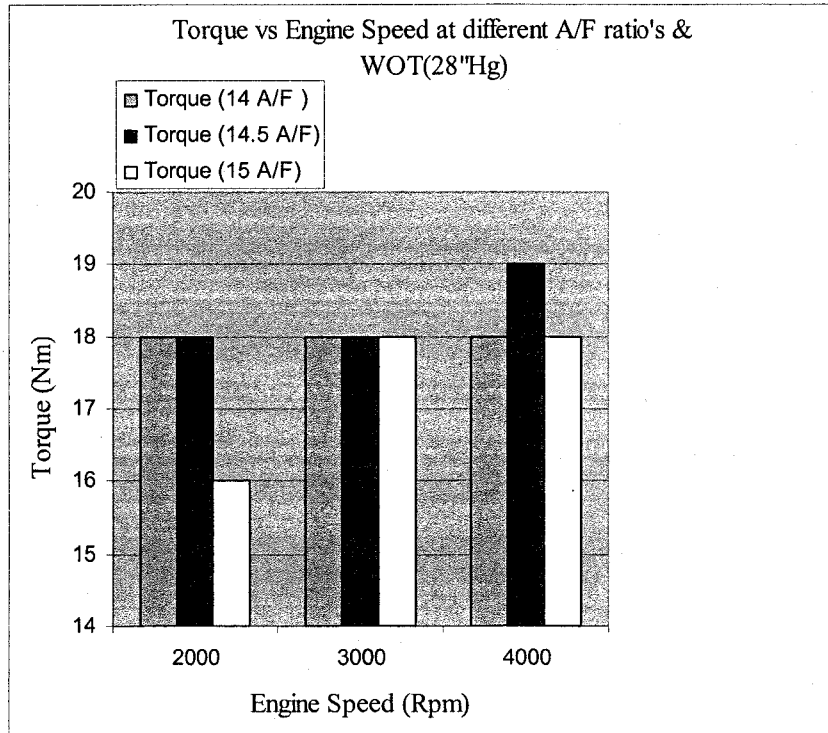


Figure 37: Comparison of torques at different speeds, different air fuel ratio's and WOT 28" Hg (natural gas)

The corresponding corrected values of torques varied from 59 -29 (Nm) for the speeds varying from 2000-4000 rpm.

2) Comparison of power output at different speeds and different air fuel ratio's carried out at wide open throttle 28" Hg.

Table 7: Different power outs at different speeds, different A/F ratio's and WOT 28" Hg
(natural gas)

Rpm	HP(1)	HP(2)	HP(3)
2000	6.85	6.85	6.09
3000	10.28	10.28	10.28
4000	13.71	14.47	13.71

Where (1) represents an lean air fuel ratio of 14

(2) represents an stoichometric air fuel ratio of 14.5

(3) represents an rich air fuel ratio of 15

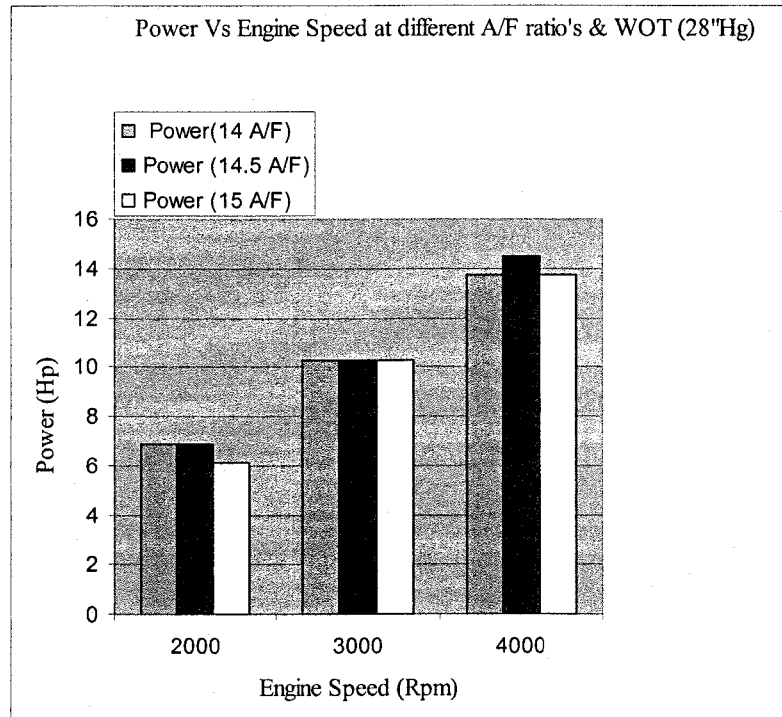


Figure 38: Comparison of power output at different speeds, different A/F ratio's and
WOT 28" Hg (natural gas)

The corresponding corrected values of horse power gave a constant value of 22.468
(Nm) for the speeds varying from 2000-4000 rpm.

Engine emission evaluation while operating it on natural gas

1) Comparison of the emissions before and after a catalytic converter at different speeds, wide open throttle 28" Hg and at stoichiometric air fuel ratio 14.5.

Table 8: Emissions observed before and after catalyst at different speeds, WOT 28" Hg and 14.5 A/F ratio (natural gas)

Rpm	CO(B)	CO(A)	No _x (B)	No _x (A)
2000	4000	175	1780	1000
3000	2500	122	1270	600
4000	4000	89	1380	450

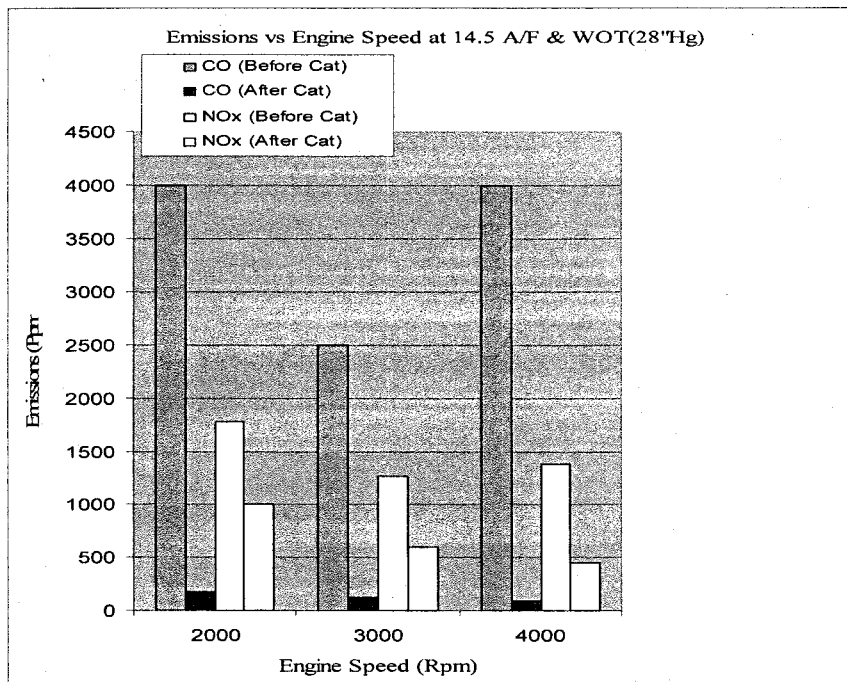


Fig 39: Comparison of emissions at different speeds, stoichiometric air fuel ratio 14.5 and WOT 28" Hg (natural gas)

It can be seen from the graph that the levels of CO and NO_x are considerably reduced after the catalytic converter.

2) Comparison of the emissions before and after a catalytic converter at different speeds, wide open throttle 28" Hg and at a lean air fuel ratio 14.

Table 9: Emissions observed before and after catalyst at different speeds, WOT 28" Hg and 14 A/F ratio (natural gas).

Rpm	CO(B)	CO(A)	No _x (B)	No _x (A)
2000	4000	600	1455	74
3000	4000	2750	1060	130
4000	4000	4000	1090	154

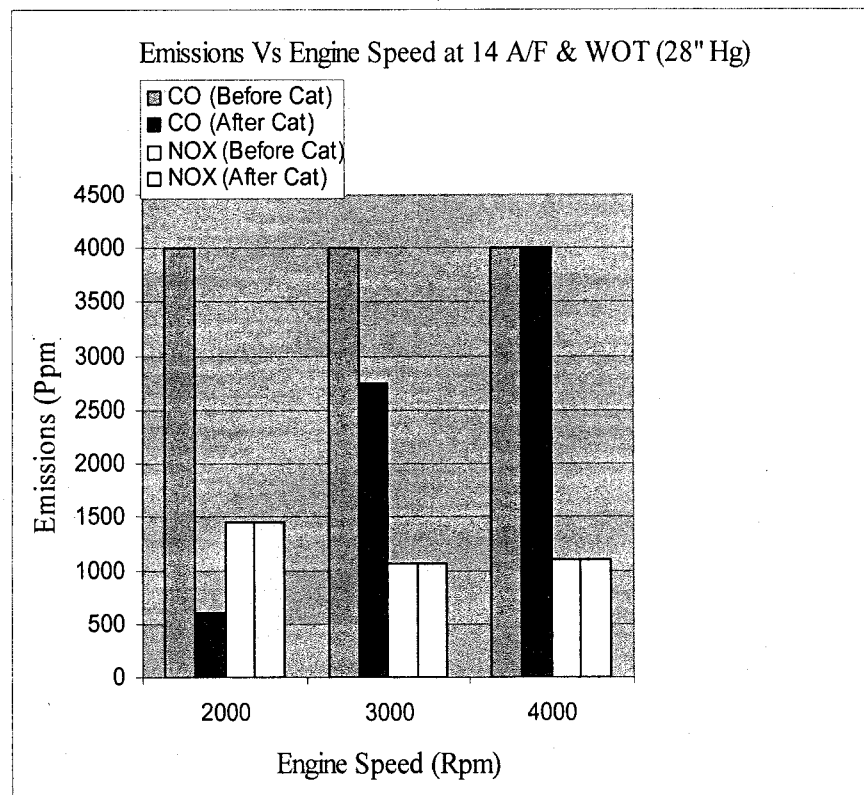


Figure 40: Comparison of emissions at different speeds, lean air fuel ratio of 14 and WOT 28" Hg (natural gas)

3) Comparison of the emissions before and after a catalytic converter at different speeds, wide open throttle and at a rich air fuel ratio 15.

Table 10: Emissions observed before and after catalyst at different speeds, WOT 28”Hg and 15 A/F ratio (natural gas)

Rpm	CO(B)	CO(A)	No _x (B)	No _x (A)
2000	3080	162	1900	1700
3000	717	70	1480	1280
4000	916	90	1720	1445

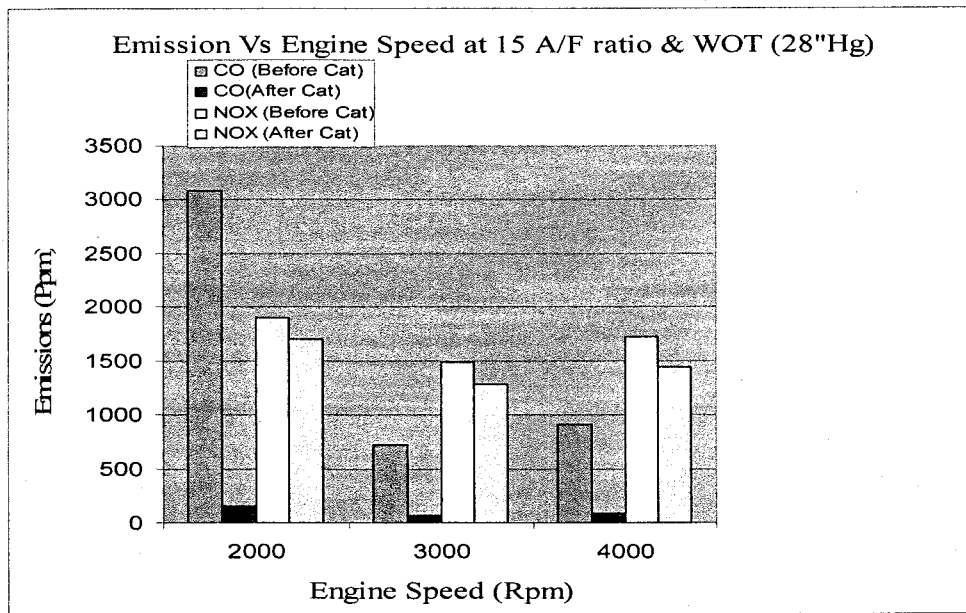


Fig 41: Comparison of emissions at different speeds, rich air fuel ratio 15 and WOT (natural gas)

A) Observation of the results obtained by running the engine in gasoline and natural gas the engine performance while running with lean A/F ratio did not result in decrease in power. This is not usually expected because generally running with a lean mixture results in lesser power output. The reason for this abnormal behavior was that O₂ sensor was working but out of required exhaust temperature levels. In short, the O₂ sensor required a minimum exhaust temperature of 300 C or approximately 572 F of which we were unable to achieve at low loads or engine speeds. Keeping the time factor in view, studies have to be pursued later for rectifying this error.

B) Emissions for CO and CO₂ for gasoline look strangely high and sometimes unchanging. These false reading we believe might be due to oil combustion or valve overlap.

Engine performance while running on hydrogen gas

C) Port Injection of Hydrogen.

Testing plans for solenoid valve, installed in the engine, consisted of operating the engine at 2000 and 3000 rpm with a load 75%. As the tuning of the engine at the rated speed of 4000 rpm was accompanied by pre-ignition, back fire and knock, it was not a good idea to operate at that speed.

1) The following results have been observed with port injection of hydrogen.

Table 11: Comparison of power output at different engine speeds and at an A/F ratio of 40:1 (port injection of hydrogen)

RPM	HP
2000	3
3000	5

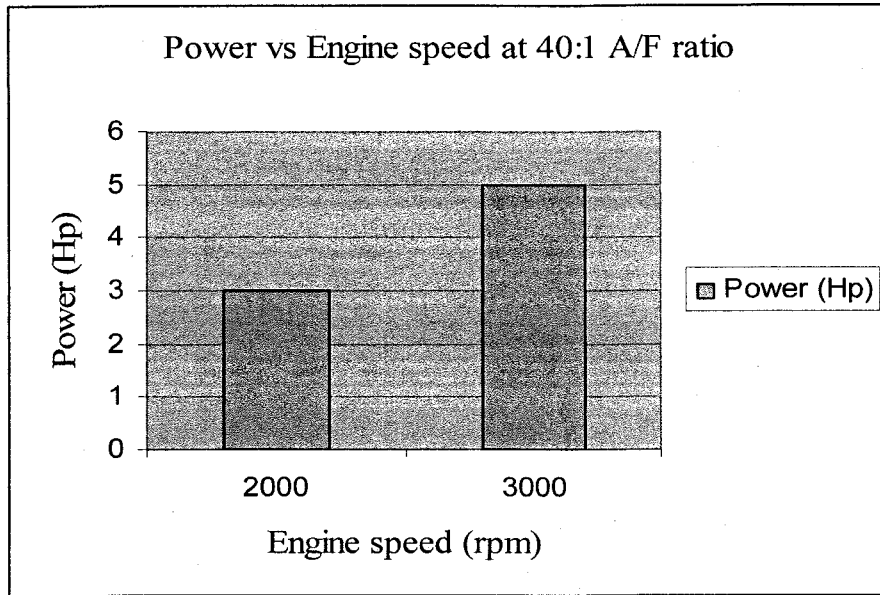


Fig 42: Comparison of power output at different engine speeds and 40:1 A/F ratio (port injection of hydrogen)

2) Table12: Comparison of torques at different engine speeds and at an A/F ratio of 40:1. (port injection of hydrogen)

RPM	Torque
2000	8
3000	10

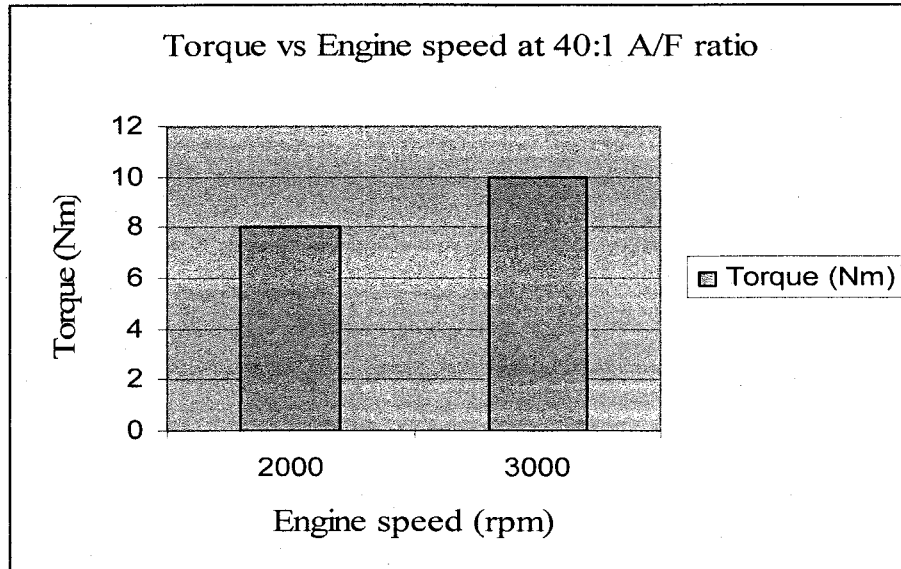


Fig 43: Comparison of Torques at different engine speeds and 40:1 A/F ratio (port injection of hydrogen)

3) Table 13: Comparison of emissions at different engine speeds and at an air fuel ratio of 40:1 (port injection of hydrogen)

Rpm	CO	NOX
2000	300	400
3000	200	160

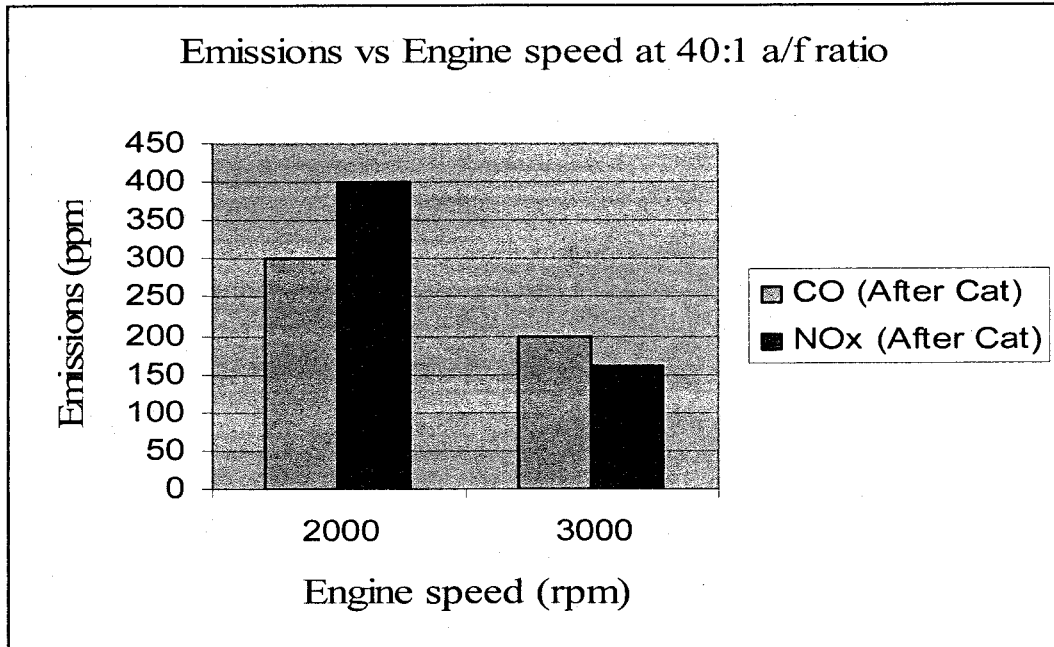


Fig 44: Comparison of emissions at different engine speeds and 40:1 A/F ratio (port injection of hydrogen)

D) Direct Injection of Hydrogen

The engine was tested to indicate a peak hp of 11.5 achieved at 32:1 slightly above stoichiometric at rated engine speed of 4000 rpm. It was a difficult task to tune the engine at the rated speed, as pre-ignition starts up.

1) Table 14: Comparison of power output at different engine speeds and 20:1 air fuel ratio (direct injection of hydrogen)

Rpm	Power (Hp)
2000	3.5
3000	7

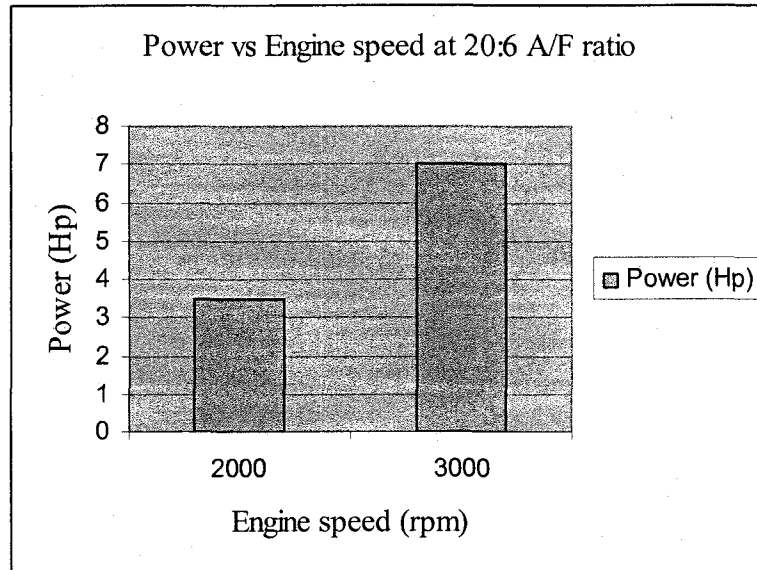


Fig 45: Comparison of power output at different engine speeds and 20.6 air fuel ratio
(direct injection of hydrogen)

2) Table 15: Comparison of torques at different engine speeds and 20:1 air fuel ratio
(direct injection of hydrogen)

Rpm	Torque (Nm)
2000	9.19
3000	12.25

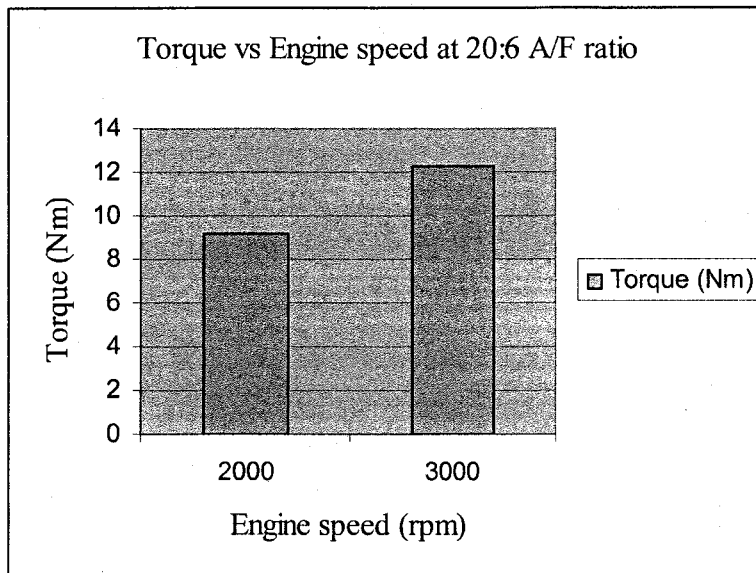


Fig 46: Comparison of torques at different engine speeds and 20.6 air fuel ratio (direct injection of hydrogen)

The engine gave out zero NO_x while running at these speeds. Thus, in-cylinder injection of hydrogen in the Polaris engine was a successful attempt in giving out zero NO_x emissions.

CHAPTER 4

SUMMARY, CONCLUSION AND DISCUSSION

Thus while running the Polaris Engine with in-cylinder injection of hydrogen, there were virtually zero NO_x emissions and a peak hp of 11.5 at rated engine speed of 4000 rpm accompanied by slightly stoichiometric A/F ratio of 32:1. Whereas, port injection gave out certain emissions with respect to CO and NO_x . While comparing the engine performance with gasoline and natural gas the values were comparatively lower than that obtained with running on hydrogen. This behavior of hydrogen pertains to larger flammability limits of hydrogen/air mixture. Thus, the engine had pre-ignition, back-fire and knock during the operation port as well as in-cylinder injection.

It can be concluded that in the near future more research has to be carried out in order to evaluate in detail the engine performance. But on the other hand, the conversion of the Polaris Ranger engine into in-cylinder injection has been a great success. In sense that we are able to convert, run the engine on hydrogen and also were able to get some performance results too.

APPENDIX I

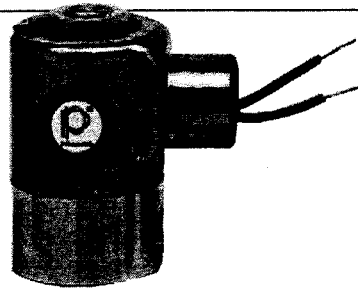
- 1) PDF of solenoid valve from Peter Paul.
- 2) PDF of booster box from Hoerbiger Company.
- 3) PDF of Hoerbiger injector.

Solenoid Valve from Peter Paul

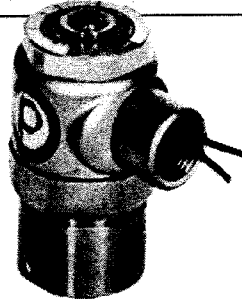


**PETER
PAUL**

**SERIES 20 MODEL H22 & EH22
2-WAY NORMALLY CLOSED HIGH PRESSURE
IMPACT TYPE SOLENOID VALVE**



H22



EH22

EXCLUSIVE FEATURES INCLUDE:

A precision stainless steel **PLUNGER** that supplies the necessary impact force to energize valve.

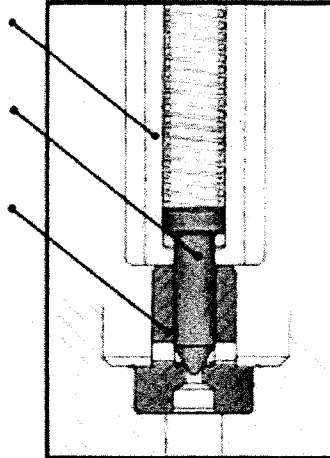
A **Kel-F* PIN†** which functions as a sealing element, that is carefully machined for maximum concentricity and fine finish.

The **ORIFICE GUIDE** is one piece, for near perfect alignment. This means bubble-tight sealing from low pressures right up to maximum pressure rating with the bonus of longer life. The one piece

Orifice/Guide can be pressed into almost any standard cavity making it available as an operator for special customer installations.

† Other pin materials available. consult factory

PATENTED



OTHER FEATURES INCLUDE:

Simple construction...

Only 2 moving parts

Available in both standard and

explosion proof construction

1/8 or 1/4 NPT ports

PRINCIPLES OF OPERATION

When the valve coil is energized, the plunger is drawn towards the sleeve end stop. The plunger is allowed to accelerate freely for a short distance before it makes contact with the pin shoulder. Upon contact it imparts considerable force on the pin causing it to lift off the seat. A return spring provides the return force, directly on the pin, to seal the orifice when the coil is de-energized.

OPTIONS AVAILABLE: - 2 WAY NORMALLY CLOSED HI-PRESSURE VALVE

HOUSING OPTIONS* - see page 78

*STRAIN RELIEF CONNECTOR

*SINGLE AUTOMOTIVE

*DOUBLE AUTOMOTIVE

*"AN" CONNECTOR

MOUNTING BRACKET

COIL OPTIONS - see page 78

MOLDED COIL

POTTED COIL & HOUSING

MISCELLANEOUS OPTIONS - see page 76

HIGH TEMPERATURE MOLDED COIL

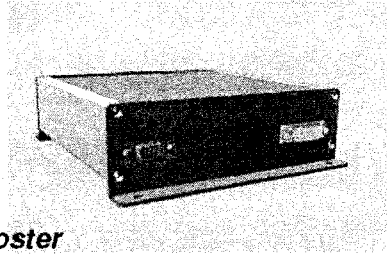
SILVER SHADING RING

ALUMINUM SHADING RING

Note: Availability of certain options or combination of options may vary with quantity of units ordered. Consult representative or factory.

*Not available with explosion proof housing

Booster Box from Hoerbiger



3-channel Valve booster

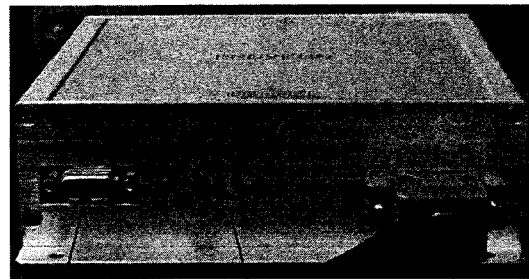
Provebo


HOERBIGER

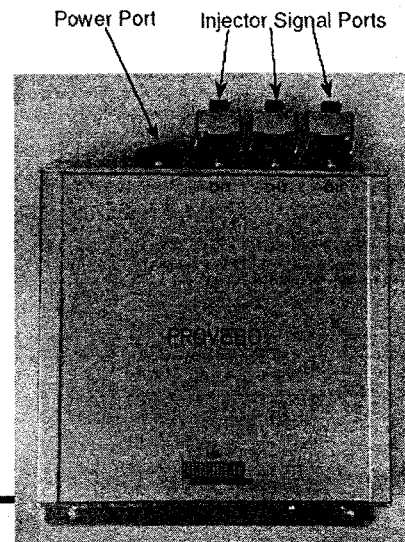


Electronic Booster

Design of Provebo Electronic Booster



PC data Port Provebo Signal LEDs Input Signal



Power Port Injector Signal Ports

Electronic Booster

Provebo Booster Settings

Parameter	Value	Unit	Note
Voltage Range	8 – 30	V	Maximum Short time Voltage 36V The injector drivers are automatically shut off above 36V and below 8V
Peak Current	0 – 20	A	Adjustable in 0,1A steps
Hold Current	0 – 10	A	Adjustable in 0,1A steps
Boost Time	0 – 2	ms	Adjustable in 10µs steps
Boost Voltage	12 – 90	V	Adjustable in 16 steps
Peak Time	0 – 10	ms	Adjustable in 50µs steps
Input Level (ON)	< 0,8	V	Internal Pull-up resistance of 3kΩ against power source
Input Level (OFF)	> 1,7	V	Internal Pull-up resistance of 3kΩ against power source


HOERBIGER

Electronic Booster

Provebo Booster LED Signals

Green LEDs light up when a open signal is given to the respective output port

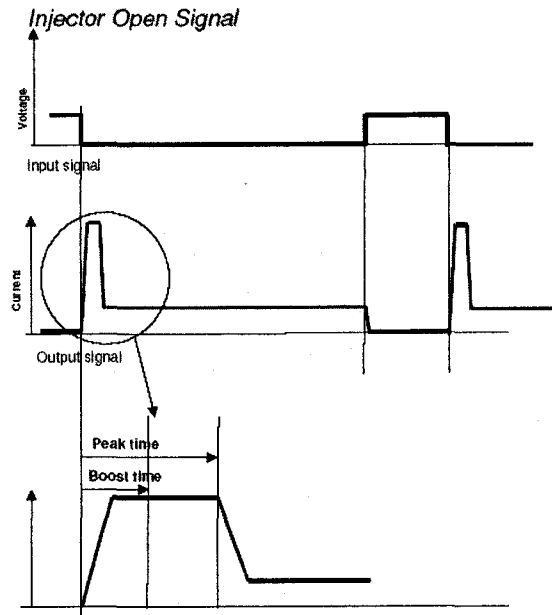
Red LEDs light up when the electronics recognizes a problem with either the injector or the cables leading to the injector.

Error signals can be generated by one or more of the following conditions

- Short circuit recognised between injector cabling and ground
- Cable break either in the injector or connecting cables
- Peek current is not being reached


HOERBIGER

Electronic Booster



Boost Time

Starts at the negative flank of the input signal and defines how long the injector is subjected to the boost voltage

Peak Time

Defined as the amount of time that the injector is subjected to the peak current

Boost Voltage

As the signal to open is given the booster applies maximum boost voltage which increase the speed at which the peak current is generated. As a result of the boost time the boost voltage decreases and so the capacitors need to rebuild the voltage before the next cycle.

Peak Current

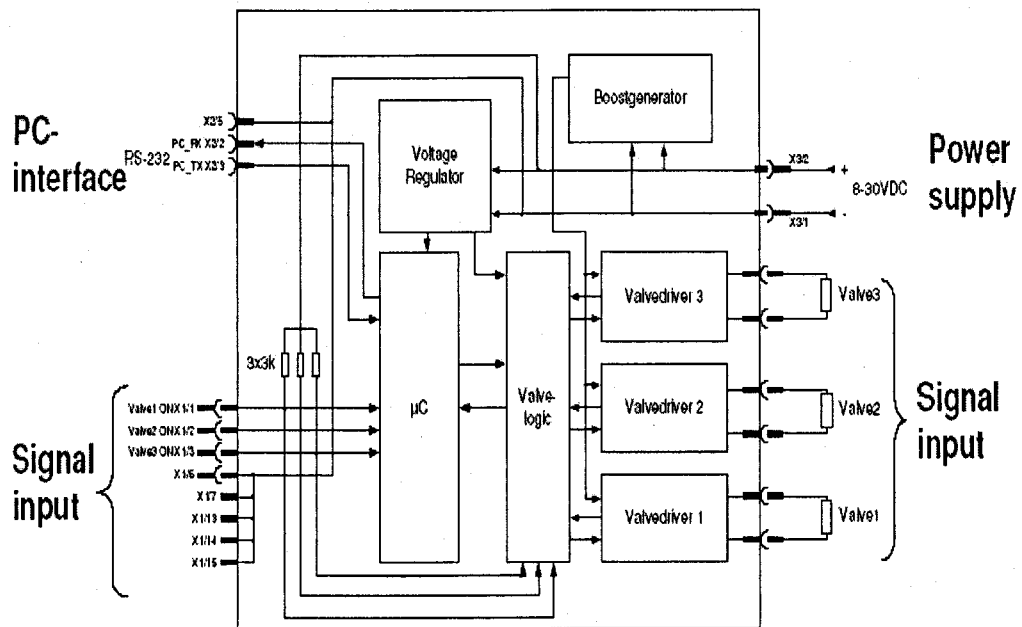
The maximum current generated during the peak time

Hold Current

The maximum current generated during the hold time

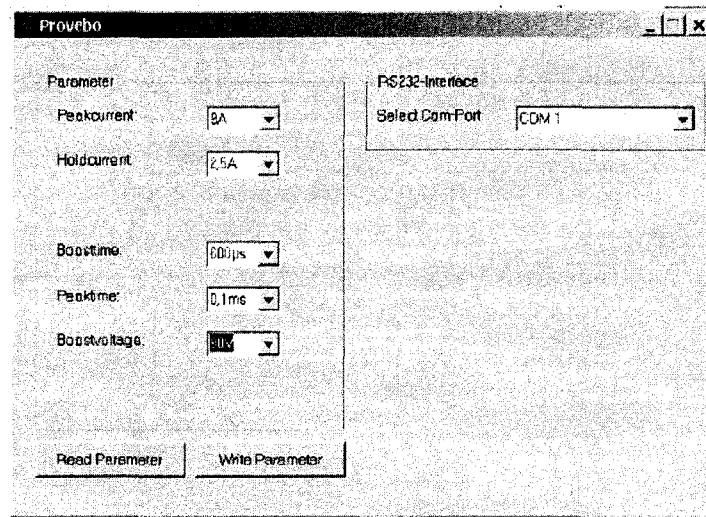

HOERBIGER

Schematic diagram



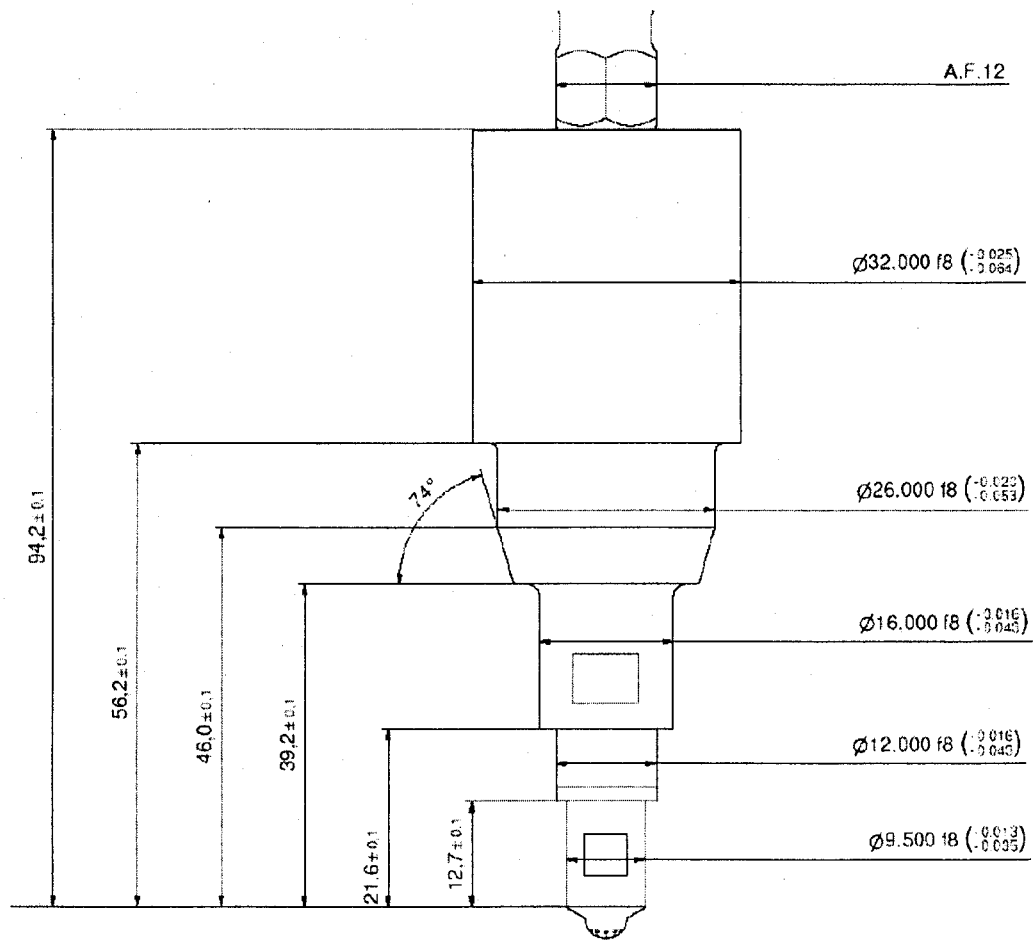

HOERBIGER

Booster Configuration Software




HOERBIGER

Hoerbiger Injector



High pressure injector

Specification for	High pressure injector
Equivalent flow area:	1.0 mm ²
Maximum intake pressure:	250 bar
Nominal intake pressure:	250 bar
Nominal discharge pressure:	50bar(g)
Steady state flow-rate at 300 K	14 g/s
Max. ambient temperature	373 K
Max. variation of flow rate	+3%
Min. Opening time:	1 ms
Response time:	~5 ms
Voltage supply	12 - 24 V
Pull-in current:	8 A
Hold-in current:	3 A
Resistance:	2 Ohm

APPENDIX II
RUN IDENTIFICATIONS

Table 16: Various test run results for gasoline carried out on 9/24/2005 around 11:30:50 am, with a total run time of 30 minutes

Rpm	Throttle Setting	Manifold Vaccum	Ignition Timing	NOX(B)	NOX(A)	CO(B)	CO(A)	Torque (Nm)	Power (Hp)	A/F
		Hg	BTDC	Ppm	Ppm	Ppm	Ppm			
2000	No Load	12"	32	350	350	1800	23	6	2.3	15.7
	Half Load	20"	28	3000	2685	4500	4000	17	6.5	
	Full Load	28"	28	4500	4000	1600	120	21	8	
3000	No Load	12"	35	273	245	2600	2350	5	1.9	15.7
	Half Load	20"	37	2600	2350	1750	141	18	10	
	Full Load	28"	37	3000	3000	1550	145	22	13	
4000	No Load	12"	37	347	331	2180	2130	5	3.8	15.7
	Half Load	20"	37	2180	2130	900	130	17	13	
	Full Load	28"	37	3700	3500	990	165	23	18	
2000	No Load	12"	32	350	108	4000	14	5	1.9	14.7
	Half Load	20"	28	2500	500	4000	97	18	6.9	
	Full Load	28"	28	2900	217	4000	670	21	8	
3000	No Load	12"	35	275	165	4000	29	4	2.3	14.7
	Half Load	20"	34	1450	152	4000	570	17	9.7	
	Full Load	28"	37	3000	450	4000	3221	22	13	
4000	No Load	12"	37	470	180	4000	48	17	13	14.7
	Half Load	20"	37	2231	290	4000	2568	18	14	
	Full Load	28"	37	3000	555	4000	4000	24	18	
2000	No Load	12"	32	363	24	4000	4000	7	2.7	13.7
	Half Load	20"	30	1850	162	4000	4000	18	6.9	
	Full Load	28"	30	2040	424	4000	4000	22	8.4	
3000	No Load	12"	35	360	35	4000	4000	7	4	13.7
	Half Load	20"	37	1757	338	4000	4000	18	10	
	Full Load	28"	37	2050	510	4000	4000	24	14	
4000	No Load	12"	37	425	6	4000	4000	7	5.3	13.7
	Half Load	20"	37	1760	431	4000	4000	18	14	
	Full Load	28"	37	2155	744	4000	4000	23	18	

Table 17 Various test run results for natural gas carried out on 10/04/2005 at 12:30:50 rpm, with a total run time of 30 minutes.

Rpm	Throttle Setting	Manifold Vaccum	Ignition Timing	NOX(B)	NOX(A)	CO(B)	CO(A)	Torque	Power	A/F
		Hg	BTDC	Ppm	Ppm	Ppm	Ppm	(Nm)	(Hp)	
2000	No Load	12"	32	59	81	1650	9	2	0.8	15
	Half Load	20"	28	979	835	2510	32	14	5.3	
	Full Load	28"	28	2009	1700	3080	162	16	6.1	
3000	No Load	12"	33	113	105	615	15	3	1.7	15
	Half Load	20"	35	750	720	1600	75	13.5	7.7	
	Full Load	28"	35	1480	1280	70	717	18	10	
4000	No Load	12"	40	203	172	580	24	5	3.8	15
	Half Load	20"	37	1010	860	1075	81	13	9.9	
	Full Load	28"	37	1720	1445	916	90	18	14	
2000	No Load	12"	32	80	33	4000	8	3	1.1	14
	Half Load	20"	28	800	70	4000	140	13	5	
	Full Load	28"	28	1455	74	4000	600	18	6.9	
3000	No Load	12"	32.5	82	38	4000	100	3	1.7	14
	Half Load	20"	35	540	27	4000	1015	13	2.8	
	Full Load	28"	35	1060	130	4000	2750	18	10	
4000	No Load	12"	40	148	12	4000	155	5	3.8	14
	Half Load	20"	37	720	87	4000	4000	14	11	
	Full Load	28"	37	1090	154	4000	4000	18	14	
2000	No Load	12"	32	101	67	3880	230	6	2.3	14.5
	Half Load	20"	28	660	530	1800	60	12	4.6	
	Full Load	28"	28	1780	1000	4000	175	18	6.9	
3000	No Load	12"	35	108	80	3370	20	4	2.3	14.5
	Half Load	20"	35	745	420	4000	100	13	7.4	
	Full Load	28"	35	1270	600	2500	122	18	10	
4000	No Load	12"	40	141	120	860	1446	4	3	14.5
	Half Load	20"	37	860	390	4000	89	13	9.9	
	Full Load	28"	37	1380	450	4000	89	19	14	

Table 18: Various test run results for hydrogen gas carried on 12/5/2005 and 4/3/2006, with a total run time of 30 minutes.

Mode of Injection	Rpm	Throttle Setting	Manifold Vaccum	Ignition Timing	NOx (A)	CO(A)	Torque	Power	A/F
			Hg	BTDC	Ppm	Ppm	(Nm)	(Hp)	
PI	2000	No Load	12"	10	400	300	8	3	40.1
	3000	No Load	12"	15	400	150	10	6	
DI	2000	No Load	12"	19	0	0	9.19	5	20.6
			12"	20	0	0	12.25	7	

Comments:

- 1) During the emission analysis, using the E-COM emission analyzer, the CO, NO_x calibration kits have been used for calibration purposes.
- 2) The abnormalities noted were sometimes very high and unchanging for CO values.

REFERENCES

1. L. S. Guo, H. B. Lu, and J. D. Li (1999) "A hydrogen injection system with solenoid valves for a four-cylinder hydrogen-fuelled engine," *IJHE*, Vol. 24, pp. 377-382.
2. I. R. Sierens and S. Verhelst (2003) "Influence of injection parameters on the efficiency and power output of the hydrogen fueled engine," *Journal of Engineering for Gas Turbines and Power* Vol 125, April 2003 pp. 444-449
3. P. C. T. DeBoer, W. J. McLean and H. S. Homan (1976) "Performance and emissions of hydrogen fueled internal combustion engines," *IJHE* Vol 1, Issue 1, pp. 153-172.
4. H. B. Mathur and P. R. Khajuria (1984), "Performance and emissions characteristics of hydrogen fueled spark ignited engines," *IJHE* Vol. 9, No8 pp. 729-735.
5. James W. Heffel, Douglas C. Johnson and Carroll Shelby (2002), "Hydrogen powered Shelby cobra: Vehicle conversion", *Hydrogen Today*, Vol 13, No 1
6. James Heffel, Andre Lanze, and Colin Messer (2001), "Hydrogen use in internal combustion engine", College of the Desert, Palm Desert, CA.
7. K. Binder and G. Withalm (1982), "Mixture formation and combustion in a hydrogen engine using hydrogen storage technology" *IJHE* Vol 7, No.8, pp. 651-659.

8. L. Martorano and D. Dini (1983), "Hydrogen injection in two –stroke reciprocating gas engines", *IJHE*, Vol 8, No 11/12, pp 935-938.
9. Helmut Eichlseder, Raymond Freymann, Jurgen Ringler, Thomas Wallner, (2003), "The potential of hydrogen internal combustion engines in a future mobility scenario", SAE International SP-1792.
10. Taku Tsujimur, Shohei Mikami et al. (2003), "A study of direct injection diesel engine fueled with hydrogen", SAE International SP-1737.
11. Xiaoguo Tan, et al. (2003), "Hydrogen IC engine boosting performance and NO_x study", SAE International SP-1743.
12. Toshio Shudo et al. (2003), "Reduction of Cooling Loss in Hydrogen Combustion by Direct Injection Stratified Charge", SAE International SP-1803.
13. Ghazi A. Karim et al. (2004), "Examination of the oil combustion in a S.I. hydrogen engine", SAE International SP-1894.
14. Andreas Wimme et al. (2005), "H₂-direct injection-A highly promising combustion concept", SAE International SP-1972.
15. Hermann Rotten Gruber et al. (2004), "Direct-injection hydrogen SI engine-operation strategy and power density potentials", SAE International SP-1902.

16. Arun K. Jaura et al. (2004), " Ford's H²RV: An industry first HEV propelled with a H₂-fueled engine - A fuel efficient and clean solution for sustainable mobility", SAE International SP-1833.

VITA
Graduate College
University of Nevada, Las Vegas
Evangeline Bulla

Home Address:

4209 Chatham Circle
Las Vegas, NV 89119

Degrees:

Bachelor of Science, Mechanical Engineering, 2002
Jawaharlal Nehru Technological University, India.

Master of Science, Mechanical Engineering, 2006
University of Nevada, Las Vegas.

Thesis Title:

The Design and Testing of A Hydrogen Fueled Internal Combustion Engine

Thesis Examination Committee:

Chairman, Robert Boehm, Ph.D, P.E.
Committee member, Yitung Chen, Ph.D.
Committee member, Ajit Roy, Ph.D.
Graduate Faculty Representative, Yahia Baghzouz, Ph.D, P.E.